

University of New Hampshire

## University of New Hampshire Scholars' Repository

---

Master's Theses and Capstones

Student Scholarship

---

Summer 2019

### AN INVESTIGATION OF NITROUS AND NITRIC ACID DIURNAL CYCLES IN BIOMASS BURNING PLUMES

Hannah Ruth Munro

*University of New Hampshire, Durham*

Follow this and additional works at: <https://scholars.unh.edu/thesis>

---

#### Recommended Citation

Munro, Hannah Ruth, "AN INVESTIGATION OF NITROUS AND NITRIC ACID DIURNAL CYCLES IN BIOMASS BURNING PLUMES" (2019). *Master's Theses and Capstones*. 1303.

<https://scholars.unh.edu/thesis/1303>

This Thesis is brought to you for free and open access by the Student Scholarship at University of New Hampshire Scholars' Repository. It has been accepted for inclusion in Master's Theses and Capstones by an authorized administrator of University of New Hampshire Scholars' Repository. For more information, please contact [Scholarly.Communication@unh.edu](mailto:Scholarly.Communication@unh.edu).

AN INVESTIGATION OF NITROUS AND NITRIC ACID DIURNAL CYCLES IN  
BIOMASS BURNING PLUMES

By

HANNAH RUTH MUNRO

Chemistry (BA), Earlham College, 2017

THESIS

Submitted to the University of New Hampshire

In Partial Fulfillment of

The Requirements for the Degree of

Masters of Science

In

Earth Science: Geochemical Systems

September, 2019

This thesis has been examined and approved in partial fulfillment of the requirements for the degree of Geochemical Systems Specialization in Earth Science by:

Thesis Director, Jack E. Dibb,  
Research Associate Professor of Tropospheric Chemistry and  
Air Snow Interface, Department of Earth Sciences,  
University of New Hampshire

Katharine A. Duderstadt,  
Research Scientist,  
Earth Systems Research Center,  
The University of New Hampshire

Meredith G. Hastings  
Associate Professor of Earth, Environmental and Planetary  
Sciences  
Brown University

On May 7<sup>th</sup>, 2019

Original approval signatures are on file with the University of New Hampshire Graduate School

## ACKNOWLEDGMENTS

I would like to thank every person involved in the completion of this thesis.

To my committee, Jack, Kathy, and Meredith. Your support, edits, and belief in my ability to complete this project were invaluable.

To my field work co-workers, Eric, Wendell, and Jiajue, I will forever remember that month we spent in Idaho, chasing wildfires, dodging endless road hazards, including but not limited to: cows, Bighorn Sheep, deer, Pronghorn etc, as well as the other wildlife we had the privilege to observe.

To the United States Forest Service, and the branches in Challis Idaho, your support of our project, guidance, and hospitality under such stressful circumstances is immensely appreciated.

To my UNH colleagues, friends, mentors, and classmates. Knowing that all of our paths had converged at that time, and we were all learning and living together, brought me a great sense of comradery.

To my friends and family, I could not have made this journey without you. You helped me along in more ways than I can write here.

Lastly, to my grandfather, you are the reason I pursued this degree in the beginning, and the reason why I perservered to the end. You will forever be my guide through the wonders of science.

Support for this research was provided through:

NOAA #NA16OAR4310099

NSF AGS #1351932

Dedicated to my grandfather, William Alexander Brown Thomson

## TABLE OF CONTENTS

ACKNOWLEDGEMENTS.....	iii
DEDICATION.....	iv
LIST OF FIGURES.....	vi
ABSTRACT.....	vii
<b>CHAPTER</b>	<b>PAGE</b>
1 INTRODUCTION	1
1.1 Reactive Nitrogen Chemisty in Wildfire Plumes	2
1.2 Description of Rabbit Foot Fire	6
1.3 Field Site	8
2 METHODS	
2.1 NOAA Van and Payload	10
2.2 HONO/HNO <sub>3</sub> Sampling	11
2.3 Sampling Stragety	12
2.4 Age Determination of Air Masses	12
3 RESULTS	13
31. Detailed Examination of 10 through 16 August	17
3.1.1 10 – 11 August	18
3.1.2 12 – 13 August	19
3.1.3 13 – 14 August	21
3.1.4 14 -15 August	24
3.1.5 15 – 16 August	26
3.1.6 Daytime Spike Camp Measurements on 16 August	28
4 DISCUSSION	30
5 CONCLUSIONS	38
6 BIBLOGRAPHY	40
7 APPENDIX	43

## LIST OF FIGURES

FIGURE		PAGE
Figure 1	Understood pathways of reactive nitrogen chemistry	5
Figure 2	Tropospheric HONO buildup at night	5
Figure 3	Rabbit Foot Fire Growth	8
Figure 4	Vegetation of the Salmon-Challis National Forest	10
Figure 5	A) MC/IC Diagram B) NOAA CSD Mobile Laboratory	12
Figure 6	Mobile Sampling Route	15
Figure 7	A) HONO & HNO <sub>3</sub> time series B) Distance from RFF while mobile	16
Figure 8	Scatter plot of HNO <sub>3</sub> vs HONO binned between day and night	17
Figure 9	August 10-11 A) Ratio of HONO/HNO <sub>3</sub> B) Time series of HONO & HNO <sub>3</sub>	18
Figure 10	August 12-13 A) Ratio of HONO/HNO <sub>3</sub> B) Time series of HONO & HNO <sub>3</sub> C) Distance from RFF	20
Figure 11	August 13-14 A) Ratio of HONO/HNO <sub>3</sub> B) Time series of HONO & HNO <sub>3</sub> C) Distance from RFF	23

Figure 12	August 14 – 15 A) Ratio of HONO/HNO <sub>3</sub> B) Time series of HONO & HNO <sub>3</sub> C) Distance from RFF	25
Figure 13	August 15-16 A) Ratio of HONO/HNO <sub>3</sub> B) Time series of HONO & HNO <sub>3</sub> C) Distance from RFF	27
Figure 14	August 16 A) Ratio of HONO/HNO <sub>3</sub> B) Time series of HONO & HNO <sub>3</sub> C) Distance from RFF	29
Figure 15	A) Emission of HONO and HNO <sub>3</sub> for burns 6-9 during FIREX 2016. B) HONO/HNO <sub>3</sub> ratio for FIREX burns 6&7	32
Figure 16	Box and Whisker plot of HONO & HNO <sub>3</sub> binned by hour	36

## **ABSTRACT:**

### **AN INVESTIGATION OF NITROUS AND NITRIC ACID DIURNAL CYCLES IN BIOMASS BURNING PLUMES**

By

Hannah Ruth Munro

University of New Hampshire, September 2019

The Western wildfire Experiment for Cloud chemistry, Aerosol absorption, and Nitrogen (WE-CAN), an NSF funded multi-platform campaign, launched with the goal of expanding scientific knowledge of the complex chemical reactions taking place inside biomass burning plumes. As a part of the WE-CAN 2018 field campaign this investigation focuses on the diurnal cycles of nitrous and nitric acid in fresh and aged smoke plumes from the Rabbit Foot Fire in the Salmon-Challis National Forest, ID. The measurements of nitrous and nitric acid in smoke plumes were made with a dual Mist Chamber/Ion Chromatograph system installed in the NOAA CSD mobile laboratory.

From these measurements we observe a clear distinction between daytime and nighttime levels of nitrous and nitric acid in smoke plumes. Nitrous acid levels peaks in the early morning hours, as high as 2ppb, and dissipates a few hours after sunrise to ~50pptv. In contrast, nitric acid levels are highest in aged smoke, 0.5 ppb, and lowest during the nighttime hours, ~20pptv. We also observe a high level of variability in individual plumes. Sample to sample concentrations of nitrous and/or nitric acid vary as much as 50%. Additionally, the two species increase both in and out of phase with one another with no distinct pattern. The ratio of the two species is a useful metric for determining the age or level of chemical processing the plume had undergone. Most

prominently, we observe the rapid production of  $\text{HNO}_3$  outpaced the production of HONO during both day- and nighttime regimes.

## CHAPTER 1: INTRODUCTION

Rising global temperatures are increasing the frequency of wildfires in the Western United States. More firestarts are the result of drier fuel sources, caused by the evaporation of larger amounts of water from leaves and soils, combined with more lightning strikes, as increasing temperature fosters the environmental conditions needed for lightning storms (Blaisdell & Lipsett, 2001). Each degree of warming is expected to correspond with a two- to four-fold increase in area burned in a wildfire (Warneke et al., 2015). It is imperative to understand the atmospheric impacts of this upsurge in wildfires and associated biomass burning (BB) in order to inform and aid fire management practices and air quality control.

The Western Wildfire Experiments in Cloud Chemistry, Aerosols, and Nitrogen (WE-CAN) project aims to fill in the gaps in our current understanding of the emissions from wildfires and their effects on air quality. From late July – August 2018 the NSF C-130 Research Aircraft completed over 100 flight hours around and through wildfire smoke plumes in California, Oregon, Washington, Idaho, Montana with the primary goals of tracking the plumes as they evolved in the first 12-24 hours after emission. Our team from the University of New Hampshire and Brown University used the NOAA CSD mobile laboratory (Coggon et al., 2016) to make ground-based measurements of the concentrations and isotopic composition of key N oxides for three weeks in August in the Salmon-Challis area, mainly sampling smoke from the Rabbit Foot Fire.

This work specifically strives to advance knowledge of formation pathways and atmospheric chemistry of oxidation products of nitrogen oxides ( $\text{NO}_x = \text{NO} + \text{NO}_2$ ) from BB emissions, using observations of nitrous acid ( $\text{HONO}$ ) and nitric acid ( $\text{HNO}_3$ ) during both day and night. Data

from this effort can be utilized to better constrain impacts of BB on air quality, as well as test current chemical mechanisms to identify potential missing reactions and reaction rates (Akagi et al., 2011). Understanding the chemistry of reactive nitrogen compounds is particularly significant because  $\text{NO}_x$  is a precursor to the atmospheric pollutant and oxidant ozone ( $\text{O}_3$ ).

The Rabbit Foot Fire observations confirm that HONO and  $\text{HNO}_3$  can serve as indicators of smoke impacted plumes in the absence of a conservative tracer. The ratios of HONO to  $\text{HNO}_3$  also provide information about chemical processing, with ratios during the day and in non-impacted airmasses remaining low ( $<1$ ), freshly impacted air masses during the day showing modest enhancements (4-6), and fresh plume ratios much higher at night ( $>10$ ). The HONO/ $\text{HNO}_3$  ratios also suggest a delay in chemical processing, with nighttime ratios persisting into early morning and daytime ratios persisting into early evening. From the variability of these ratios, there is some evidence of net production of  $\text{HNO}_3$  at night in the absence of photochemistry. Variability over short time scales also suggest significant heterogeneity caused by terrain and local meteorology.

### **1.1. Reactive Nitrogen Chemistry in Wildfire Plumes**

Numerous studies have been conducted to characterize the compounds released in wildfires, using both fuel specific and non-specific BB to understand the effects increased emissions will have on our atmosphere. Some of the most recent efforts include the SEAC4RS field campaign in 2013 and the lab experiments FLAME-4 in 2012 and FIREX-FIRELAB in 2016. FIREX was a collaborative effort between the National Oceanic and Atmospheric administration (NOAA) and the USDA Fire Science Laboratory in Missoula, MT (US Department of Commerce). The study aimed to improve the current working knowledge of “emissions and short timescale processing” and focused primarily on fuels representative of wildfires in western North America.

These experiments confirmed that the smoke emitted from BB is chemically complex. It is primarily composed of carbon dioxide, water vapor, carbon monoxide, particulate matter, hydrocarbons, and trace minerals; but contains thousands of other compounds (Bytnerowicz et al., 2016; Veres et al., 2010). The specific ratios of the components emitted are dependent on the fuel types burned. Some of the most important primary emissions from BB are the reactive nitrogen species ( $\text{NO}_x$  and HONO) and non-methane organic carbons (NMOC) (Benedict et al., 2017; Nie et al., 2015). Secondary emissions form from the interactions of NMOC,  $\text{NO}_x$ , water vapor, and sunlight and include  $\text{HNO}_3$ , peroxyacetyl Nitrates (PANs), and particulate nitrate (p- $\text{NO}_3$ ). Other components of the smoke plume are gaseous and aerosol compounds including but not limited to black carbon (BC), brown carbon (BrC), volatile organic compounds (VOC), semi-volatile organic compounds, and mineral dust. These particles can enhance secondary production of HONO through heterogeneous reactions of  $\text{NO}_2$  and water (Akagi et al., 2012).

Our study focuses on the nitrogen compounds, specifically nitrous acid (HONO) and nitric acid ( $\text{HNO}_3$ ). These compounds react with other emitted species to produce ozone ( $\text{O}_3$ ) in the troposphere.  $\text{O}_3$  is considered a health hazard, and increasing wildfire occurrences can lead to  $\text{O}_3$  concentrations in remote regions exceeding National Ambient Air Quality standards (US EPA). Tropospheric  $\text{O}_3$  levels as low as 40 ppb are associated with crop damage.  $\text{O}_3$  is also considered a human health hazard, as it irritates the lungs and can inflame the respiratory pathway. Nitric Acid is phytotoxic to sensitive vegetation as well. (Bytnerowicz et al., 2016).

The complex reactions of  $\text{NO}_x$  and HONO depend on several atmospheric factors including diurnal variability. Our current understanding of the daytime chemistry of reactive nitrogen species is summarized in Figure 1. The photolysis of  $\text{O}_3$  (not shown in Figure 1), HONO, and several other species including oxygenated volatile organic compounds (OVOCs)

provides an initial source of the hydroxyl radical (OH), one of the most important oxidants in the daytime atmosphere (Ren et al., 2013). The fast NO<sub>x</sub> cycle in the atmosphere is kickstarted by the reaction between O<sub>3</sub> and NO (Figure 1). VOCs oxidize to form peroxy radicals (HO<sub>2</sub> and RO<sub>2</sub>) which convert NO to NO<sub>2</sub> without consuming O<sub>3</sub>, resulting in the net production of O<sub>3</sub> (Jaffe & Wigder, 2012). While NO<sub>x</sub> is cycling back and forth, NO is also reacting with OH radicals to form HONO. HONO rapidly photolyzes back to NO and OH during the day and plays an important role as an atmospheric oxidant, especially in polluted areas. Studies have found that the HONO to CO ratio decreases downwind of daytime fires, sometimes by as much as a factor of 10 over a period of 20 minutes, implying that the loss of HONO far outweighs its production in daytime plumes (Palm et al., 2017). Heterogenous reactions remain one of the least understood pathways in HONO production, as discussed in Nie et al. (2015). HNO<sub>3</sub> is primarily formed through the reaction of NO<sub>2</sub> and OH. HNO<sub>3</sub> is considered a terminal species and a sink for NO<sub>x</sub> and usually is rained out from the atmosphere.

The daytime chemistry of reactive nitrogen species is well understood, in part because it is easier to measure emissions during the day due to flight restrictions. However, it is important to have an equivalent understanding of the chemical pathways occurring in nighttime smoke plumes, as they reside in the boundary layer and have large impacts on local surface air quality. The lack of photolysis at night does not necessarily equate to a lack of chemical reactivity. At night, plume chemistry changes dramatically as the photolysis of NO<sub>2</sub> to NO ceases, interrupting the fast NO<sub>x</sub> cycle. HONO and the NO<sub>3</sub> radical also build up in the atmosphere (Figure 2). The NO<sub>3</sub> radical is formed by the reaction of NO<sub>2</sub> with O<sub>3</sub> and reacts with additional NO<sub>2</sub> to produce dinitrogen pentoxide (N<sub>2</sub>O<sub>5</sub>). N<sub>2</sub>O<sub>5</sub> and water on aerosol react to form HNO<sub>3</sub> along with other nitrate aerosols, both of which act as a terminal sink for NO<sub>x</sub>. HONO stays in the atmosphere

until sunrise the next day and photolyzes to kickstart the  $\text{NO}_x$  pathway again. The  $\text{NO}_3$  radical photolyzes even faster than HONO when the sun returns, so production of  $\text{N}_2\text{O}_5$  becomes insignificant, and residual  $\text{N}_2\text{O}_5$  thermally decomposes as temperatures rise during the day. Heterogeneous reactions of  $\text{NO}_2$  plus water on aerosol and other surfaces are potentially important sources of nocturnal HONO but cannot support the levels of daytime measured HONO (Nie et al., 2015). Note, these reactions are not shown in Figure 1.

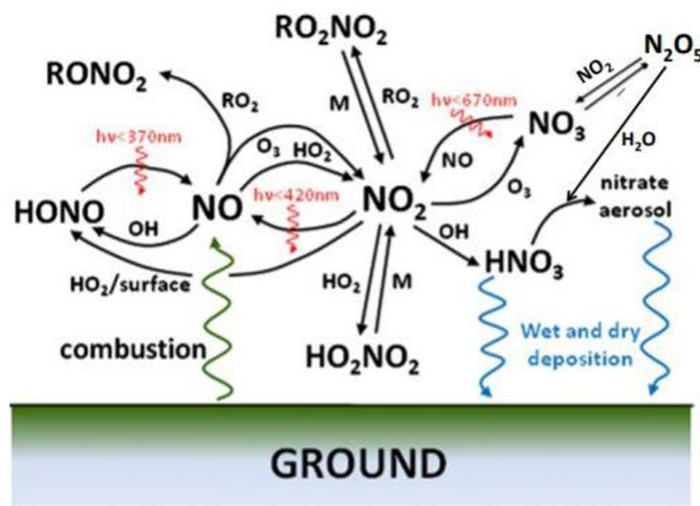


Figure 1: A summary of the currently understood pathways of reactive nitrogen chemistry in smoke plumes. Of note are the reactions that require input of photochemical energy.  $\text{HONO} \rightarrow \text{NO}$ ,  $\text{NO}_2 \rightarrow \text{NO}$ , and  $\text{NO}_3 \rightarrow \text{NO}_2$ . (“Statement of Work,” 2016.)

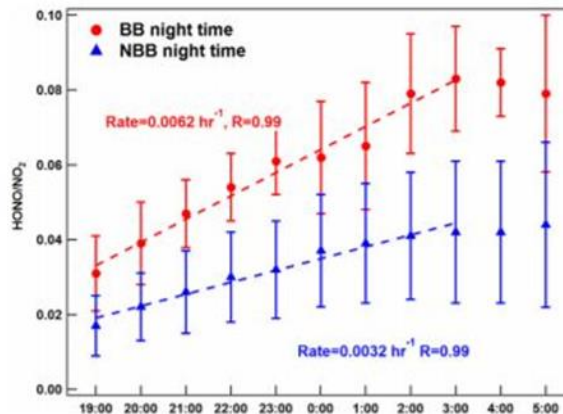


Figure 2: HONO buildup at night in the troposphere (Nie et al., 2015)

## 1.2 Description of the Rabbit Foot Fire

Figure 3 shows the evolution and extent of the Rabbit Foot Fire (RFF), initially detected on 2 August 2018 at 12:30 pm local time (MDT) at 44.856°N, 114.307°W, in the Salmon-Challis National Forest. Over the next several days the fire grew NE from 600 to 2,300 acres by 6 August (Figure 3). The fire was burning in a mixed conifer forest primarily composed of lodgepole pine and douglas fir, interspersed with subalpine fir and whitebark pine. Torching, spotting, and running behavior were observed. The RFF was more active on 7 August than the previous days and grew in two different directions; southwest and towards the northeast (Figure 3). On 7 August the Spike Camp was established by the local Forest Service for overnight monitoring of the fire and ease of travel for the firefighters. This was in part because the fire was beginning more rapid growth and was still uncontained. On 8 August the southern lobe of the RFF overran the previous fire perimeter, growing to the southeast to 4,339 acres. A similar trend in fire spread and growth occurred on 9 August; gaining 1,300 acres, for a total size of 5,645 acres, and continuing its southbound track. Due to shifting winds and hot dry conditions, the RFF grew to 6,357 acres on 10 August and continued to burn actively along its northeast edge, burning pockets of unburnt fuel within its perimeter. We began to actively measure the emissions from the RFF at this time.

The winds shifted again on 11 August, pushing the fire towards the Northeast (the larger “finger”) and grew to 7,542 acres. Large fire growth occurred on 12 August, gaining almost 3,000 acres spreading north as well as south, further extending the fire perimeter. The RFF experienced active burning throughout the day, and large plumes were visible for several miles. The next day, 13 August, saw large growth upwards of 8,000 acres on the NE corner of the RFF.

Fire conditions were reported as extreme, preventing combative efforts on the NE edge. Columns of smoke continued to be visible throughout the day and into the evening. Continuous burning throughout the day of 14 August resulted in 3,200 acres growth on the eastern flank of the RFF, and by 15 August the total burned area reached 26,294. The fire grew again on 17 August to a total of 34,201 acres. Passing thunderstorms with lightning caused several new points of ignition within the pre-existing perimeter of the RFF. We left the area on 17 August and started the trip back to Missoula.

We were able to sample emission from several of the days of large growth during our mobile measurements. The nights of the 12–13 August 13–14 August, and 14–15 August are all time intervals of interest because of the expansion of the RFF associated with those days. The RFF continued to burn and grow until October. One of the last updates occurred on 1 October and reported 36,004 acres burned at 20% containment. The final update on 13 November reported minimal fire activity with continued monitoring of isolated smoke plumes (USDA Forest Service).

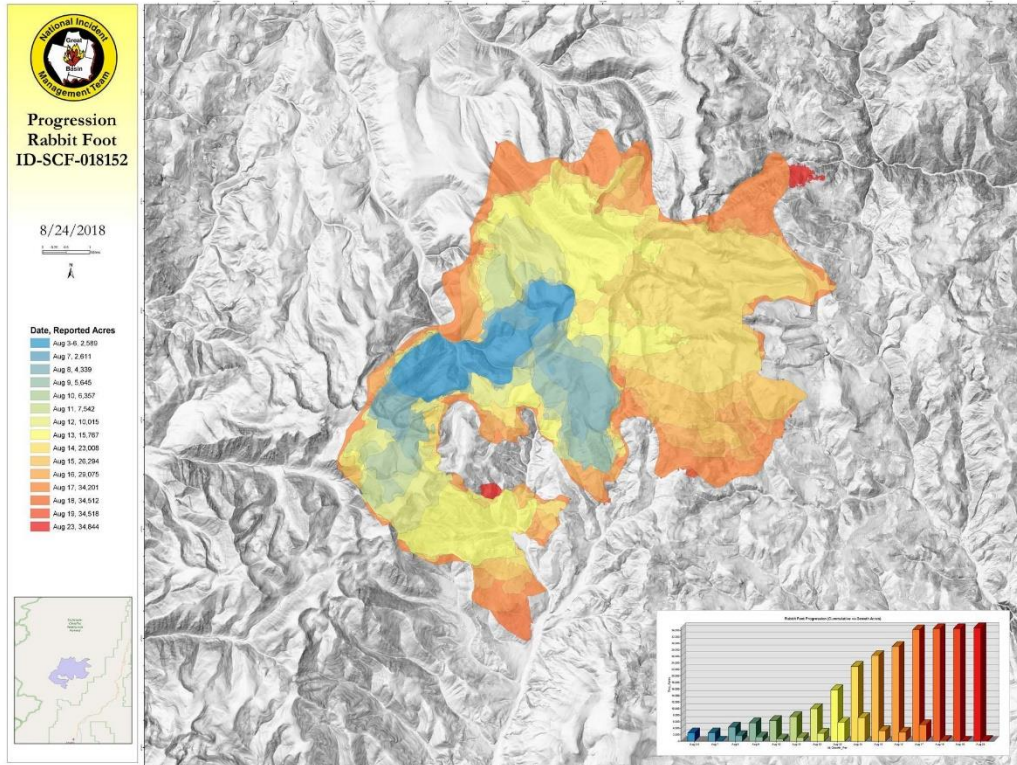


Figure 3: Map of the growth of the Rabbit Foot Fire from 2 August through 23 August. Colors are coded to represent the growth on a day, as seen in the key. Days of interest include the growth from 12 August to 16 August, light green yellow – dark orange (“Salmon-Challis National Forest - Fire Management,” 2019)

### 1.3 Field Site

The Challis Salmon National Forest in eastern-central Idaho covers 4.3 million acres. The current reserve is a conglomeration of the 1906 Salmon River Forest Reserve and the 1980 Frank Church River of No Return Wilderness. The two were combined in 1996 by the National Forest Service, and today the USDA maintains 6 districts: The Challis-Yankee Fork RD, the Middle Fork RD, Lost River RD, Salmon-Cobalt RD, the North Fork RD, and Leadore RD (“Salmon-Challis National Forest - About the Forest,” 2019). The area is highly mountainous and is dominated by Douglas Fir and Lodgepole Pine, with Spruce and Fir trees dominating higher altitudes, and Ponderosa Pine trees dominating lower altitudes (Figure 4). Grassy meadows and treeless slopes interrupt the forested areas. The Salmon River runs through 136.7 km of the

National Forest (“Salmon-Challis National Forest - National Forest Foundation”). This research was completed in the Challis area of the Salmon Challis National Forest targeting the Rabbit Foot Fire of 2018 (Figure 4). Wildfires in this area are primarily started naturally, with the average fire season encompassing several small fires, < 1 acre, and a few large ones (“Salmon-Challis National Forest - National Forest Foundation,” 2019). Fuels burned are primarily composed of Lodgepole Pine, Douglas Fir, and various sub-alpine scrubs and brush (Figure 4, “Salmon-Challis National Forest - Home,”) Weather conditions for the duration of the field campaign were hot and dry, with daily temperatures consistently in the high eighties, and reaching into the low hundreds. There was no rain during the campaign.

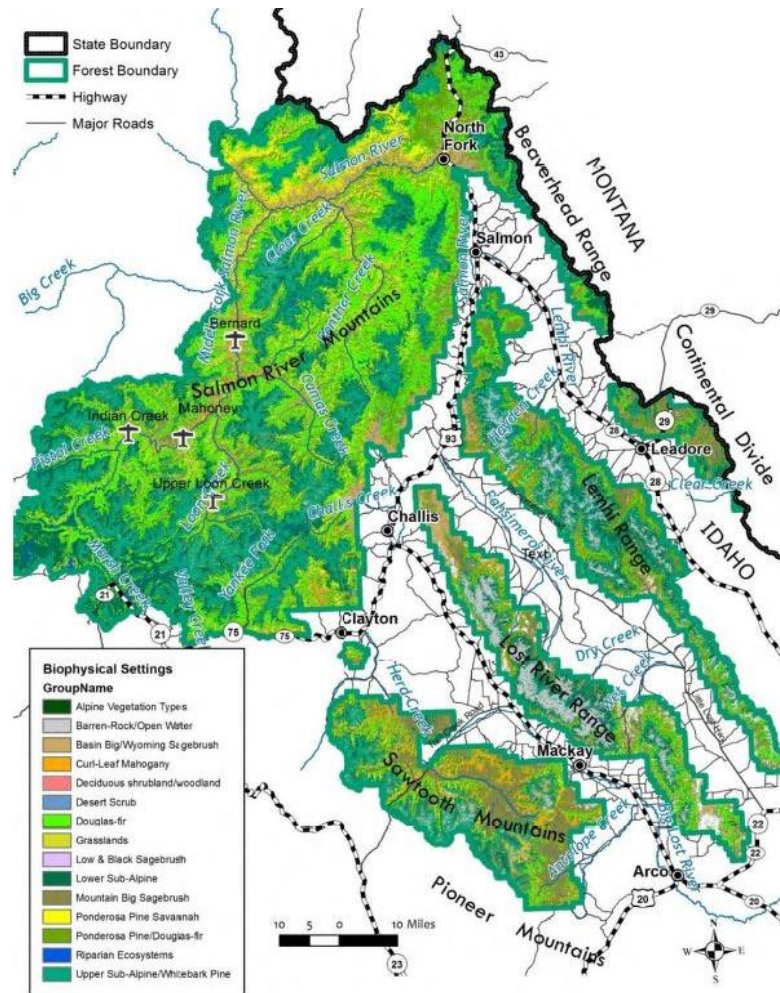


Figure 4: Vegetation types found in the Study Site, Challis, Mackay, North Fork, and Salmon ID (USDA Forest Service)

## CHAPTER 2: METHODS

### 2.1 NOAA Van and Payload

Our measurements were conducted in the NOAA mobile laboratory, described in Coggon M et al. (2016). The total payload in the van for the WE-CAN 2018 campaign included the University of New Hampshire's mist chamber / ion chromatograph (MC/IC) system for measuring HONO and HNO<sub>3</sub>; Brown University's NO<sub>x</sub> box and denuder for measuring NO<sub>x</sub>, NO and NO<sub>2</sub> (Miller, Wojtal, Clark, & Hastings, 2017); NOAA meteorological instrumentation that

measured wind speed, wind direction, temperature, relative humidity, latitude and longitude as described in Coggon M. et al. (2016); the NOAA Piccaro for measuring CO, N<sub>2</sub>O, and H<sub>2</sub>O (described in Peischl et al. 2012, 2013); a greenhouse gas analyzer from Los Gatos Research (LGR) for measuring CO<sub>2</sub>, methane (CH<sub>4</sub>), and water vapor (H<sub>2</sub>O) (Lin et al., 2018). The LGR and Piccaro instruments ran only when the van was parked and plugged into an external power source.

## **2.2 HONO/HNO<sub>3</sub> Sampling**

Gas phase sampling of HONO and HNO<sub>3</sub> was completed using a two channel mistchamber/ion chromatograph system (MC/IC) (Figure 5A) installed in the NOAA mobile laboratory (Figure 5B). Air was pulled through a single 1.27 cm OD PFA tubing inlet with an aerosol prefilter via a scroll pump. Simultaneous samples integrating over 5 minutes were collected into both MC samplers, with air flow controlled at the nominal rate of 35 L/min by independent mass flow controllers on each sampler. The mist induced by the sample air flow in the mist chamber efficiently collects water-soluble compounds in a small amount of ultrapure water (Keene et al., 1989; Talbot, et al., 1990). Fourteen mL of Millipore 18-ohm water was utilized in both mist chambers. After the 5 minutes of misting the final volume of the liquid was ~10-12 mL. Final water volume was determined by spiking the feed water with Trifluoroacetic acid (TFA). The sample solutions were removed using computer-controlled syringe pumps, with one sample immediately injected into an IC for near-real-time analysis, as described in Stutz et al. (2010). The sample from the other MC was transferred to an amber polyethylene bottle for isotopic analysis at Brown after the campaign. Nitrogen and oxygen isotopes were analyzed to track formation pathways of HONO and HNO<sub>3</sub>. Uncertainty in the MC/IC measurements of HONO and HNO<sub>3</sub> concentration is around 25%.

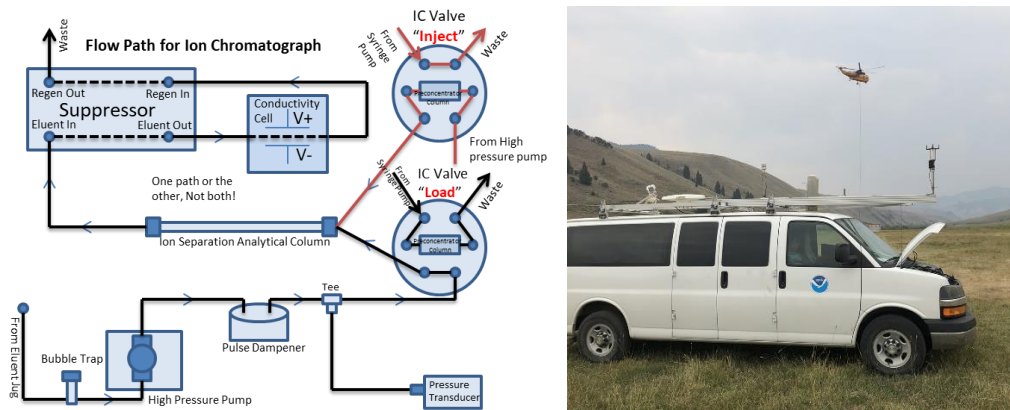


Figure 5: A) Diagram of the flow path in the MC/IC system. B) Picture of the NOAA CSD Mobile Laboratory at Spike Camp.

### 2.3 Sampling Strategy

Measurements alternated between intervals when the van was parked and plugged into grid power, and periods of mobile sampling reliant on the battery/inverter system powered by the vans two alternators. Stationary measurements allowed the use of the LGR and Piccaro instruments, while mobile measurements were restricted to Brown’s Denuders and real time  $\text{NO}_x$  monitor, the UNH MC/IC, and the MET data. Locations for stationary sampling were picked based on proximity to the Rabbit Foot Fire and the availability of RV sites with adequate power for our needs (two 30-amp outlets).

### 2.4 Age Determination of Air Masses

To determine the age of the air mass sampled by the MC/IC, the GPS coordinates from the NOAA CSD meteorological system for the van were used in conjunction with the coordinates of starting point of the RFF. These two values were input to the haversine function, calculating the distance between the van and the fire start considering the curvature of the earth. The corresponding windspeed was then used to calculate the approximate age of the air mass. This calculation provides a qualitative estimate of age, such as young, somewhat aged, aged, and

very old. The high variability of the terrain introduced a large amount of error in this calculation, contributing to the calculation of excessively long air mass travel times. As we were unable to precisely define the age of each plume, we are using these methods only to determine rough age in order to distinguish between fresh and aged plumes.

Wind direction was reported in degrees, which were converted to cardinal directions for ease of interpretation. The approximate age and wind direction were then used to determine the source of the air mass sampled, which fire it was mostly likely impacted by, and roughly how long the air mass took to get to the NOAA CSD van.

### CHAPTER 3: RESULTS

The following section provides a description of the ground-based measurement campaign, including the location and movements of the mobile lab in relation to the RFF as well as highlights of notable trends and peaks in HONO, HNO<sub>3</sub> and the HONO/HNO<sub>3</sub> ratio. The map in Figure 6 provides the context to discuss measurement location. Figure 8 presents a summary of observations from 8–16 August, including HONO (blue) and HNO<sub>3</sub> (red) in the top plot and distance from the starting location of the RFF on the bottom plot. Figure 8 shows a correlation plot of HONO and HNO<sub>3</sub> for early morning (blue) and midday (orange) sampling times for the entire period of observation. Figures 10-15 provide more detailed information of HONO, HNO<sub>3</sub> and the HONO/HNO<sub>3</sub> ratios for specific sampling intervals. Readers are referred to Appendix A for a thorough discussion of the daily measurements and more specific discussion of factors influencing the measurements.

Our first interception of smoke from the RFF occurred in Challis, ID, where we stayed briefly (7–8 of August), before moving to Mackay, ID (Figures 4 and 6). Although some smoke

impacts were present in the data at Mackay, the RFF was too far (~100 km) away to confidently say that fire was the source of the emissions. We moved again on the afternoon of 9 August to North Fork, ID to gain better proximity to the RFF (Figure 4). On the morning of the 12<sup>th</sup> of August, we relocated to the Royal Gorge resort just north of Ellis, ID (Figures 4 and 6) and used this resort as a base from which to launch a series of mobile sampling legs for the rest of the study. These mobile trips were between Salmon and Challis and up several Forest Service roads near Ellis (Figure 6). The Morgan Creek Road (MCR) turned out to afford the closest approach to the fire, and was traversed seven times, including one trip all the way to the Spike Camp (Figure 6) Distance between the van and the location where the Rabbit Foot Fire started is shown in Figure 8b, with MCR visits accounting for all intervals when we sampled < 21 km from the initiation site of the fire.

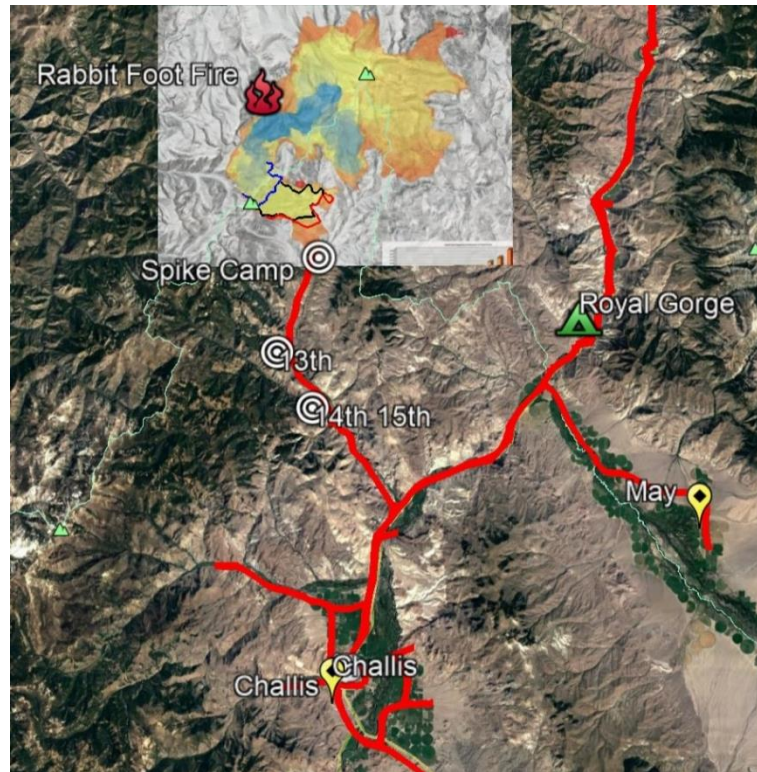


*Figure 6: Map of a subset the path of travel for the NOAA van during the WE-CAN 2018 campaign. Of note are important dates, which give the locations of the different approaches to the RFF during mobile measurements up MCR.*

Every time the van climbed MCR, we measured HONO concentrations in excess of 500 pptv (Figure 7). HONO concentrations only exceeded this 500 pptv threshold while sampling up MCR, and for several short intervals when the van was sampling along ID-93 and passed the intersection with MCR. Nitrous acid concentrations greater than 1 ppbv were observed for 30-90-minute intervals three times when the van was far up MCR; around sunrise on 13 August, and in the morning of 15 August from 3:00-4:30 and again 6:00-7:30 (Figure 7A). During full daylight hours HONO was generally  $\ll$  100 pptv except for smoke impacted plumes that could contain up to 800 pptv for short periods of time. Nitric acid was modestly enhanced in most of the smoke plumes that contained HONO greater than 500 pptv, with the notable exception of the smoke sampled up MCR in the morning of 13 August (Figure 7). However,  $\text{HNO}_3$

concentrations generally increased to at least 100 pptv from late morning to afternoon (10:00-16:00), as high, or higher than the enhancements seen in the thick smoke plumes in the early morning hours. Smoke sampled in the afternoons of 14 August and 15 August contained  $\text{HNO}_3$  concentrations  $> 200$  ppt (Figure 7A).  $\text{HNO}_3$  showed a clear diurnal variation, with lowest concentrations occurring during the nighttime hours and highest during mid-day into the late afternoon.

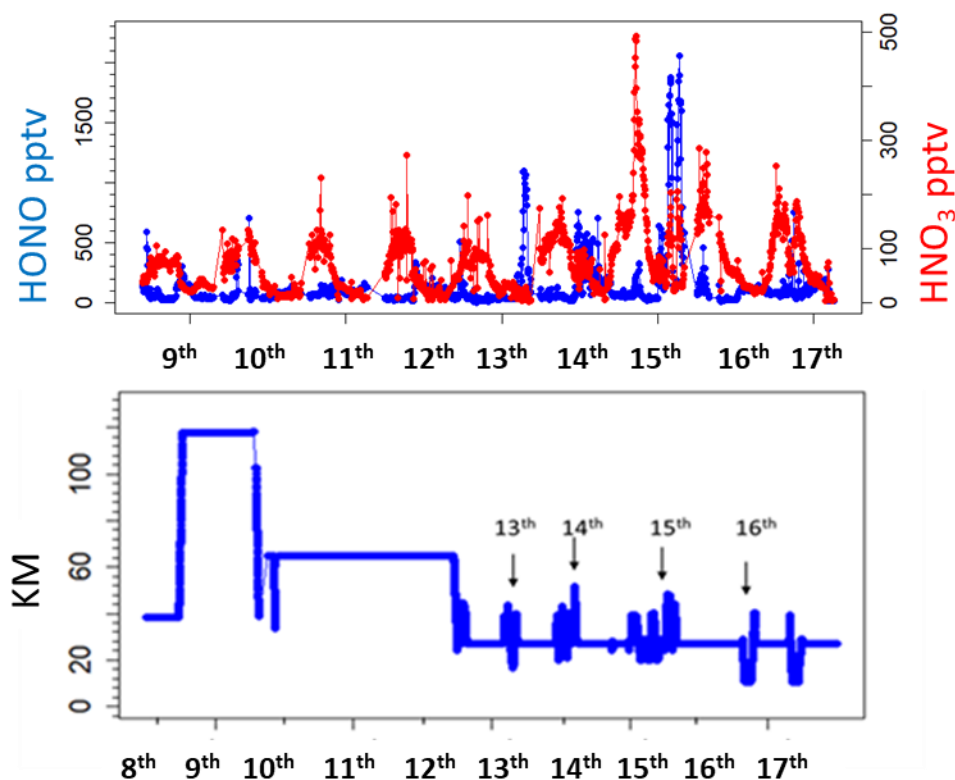


Figure 7: A)  $\text{HONO}$  and  $\text{HNO}_3$  plotted from the 10–16 August 2018. This figure encompasses the intervals of interest from the campaign.  $\text{HONO}$ , shown in blue, varies between 10 pptv–2000 pptv.  $\text{HNO}_3$ , shown in red, varies between 5 pptv and 500 pptv. Note that  $\text{HONO}$  and  $\text{HNO}_3$  concentrations are plotted on different y-axis. B) Distance from the RFF during the period of measurements from the 8th–16th. Important mobile measurements are pointed out, specifically the mornings of 13 August, 14 August, and 15 August and the daytime of 16 August.

The tendency for  $\text{HNO}_3$  to be modestly enhanced under strong sunlight and HONO to be highest in the dark creates a marked diurnal variation in the HONO/ $\text{HNO}_3$  ratio. (Figure 8). From midnight until just before sunrise this ratio was nearly constant between 7 and 10. When the sun was high the ratio decreased to levels as low as 0.1 but was much more variable.

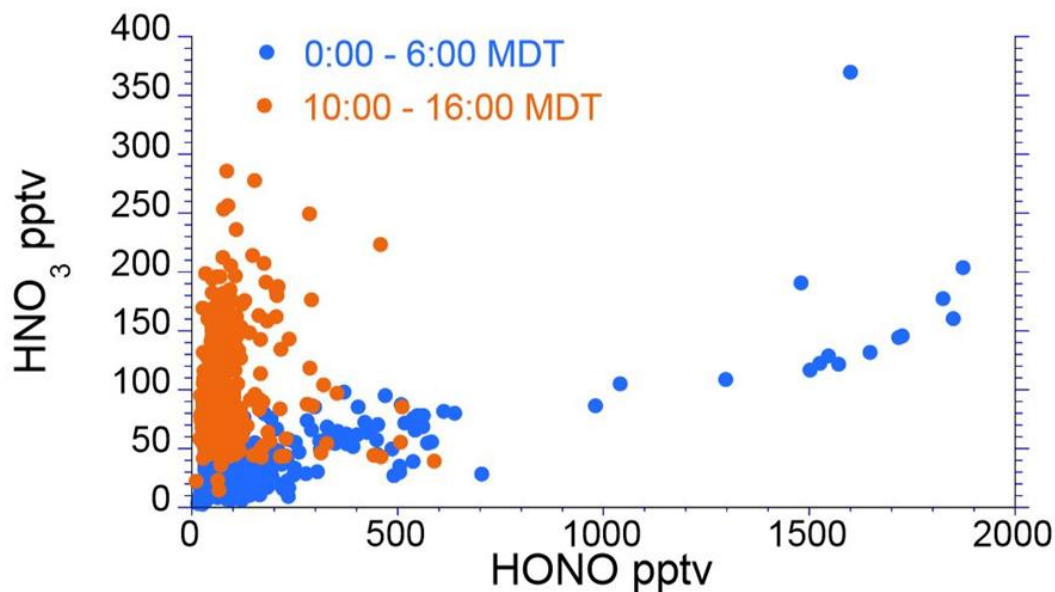


Figure 8: Scatter plot of  $\text{HNO}_3$  vs HONO binned between 6 dark early morning hours (blue) and 6 midday hours of strong sunlight (red).

The intervals used in Figure 9 are representative of the darkest night and brightest day hours and exclude time intervals that contain dusk and dawn hours to highlight the distinct partitioning of the species.

### 3.1 Detailed Examination of 10 through 16 August

Following are highlights from specific sampling intervals presented in Figures 9-14.

Appendix A provides a more thorough description of location of the mobile lab, smoke visibility, instrument details, and behavior of HONO,  $\text{HNO}_3$ , and the HONO/ $\text{HNO}_3$  ratios.

### 3.1.1 10 – 11 August

Stationary sampling took place at Wagon Hammer RV Park in North Fork ID from 10–12 August, 70 km North of the RFF (Figure 9). During this time the prevailing winds blew from the NE and we sampled a relatively old air mass.

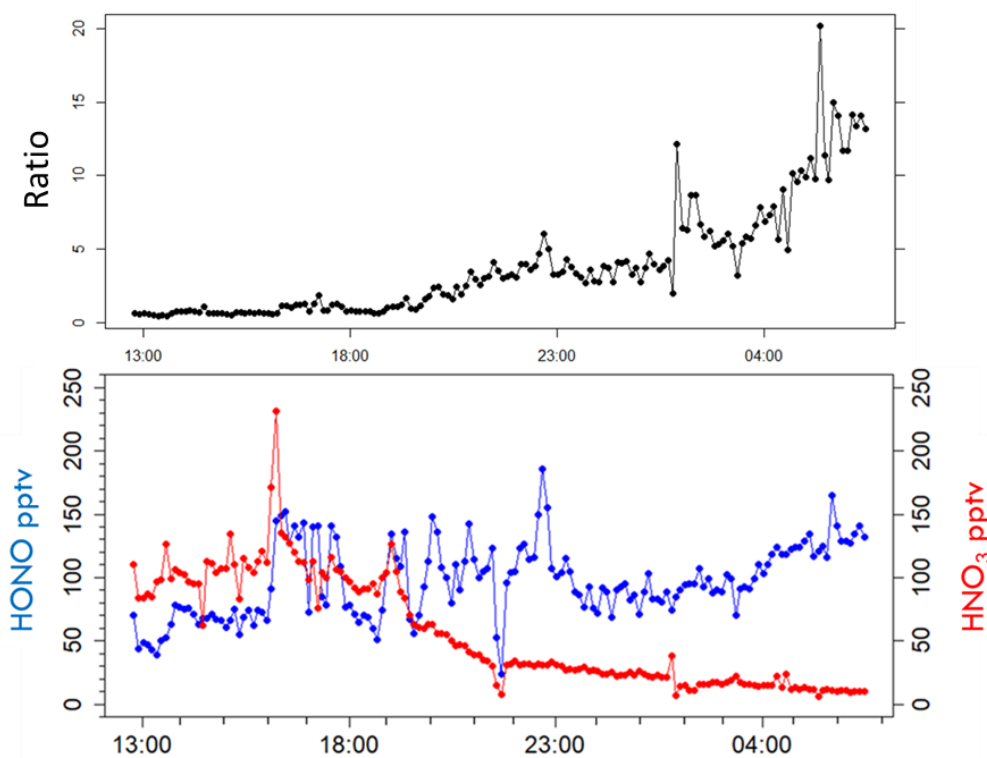


Figure 9: A) Ratio of HONO vs  $\text{HNO}_3$  plotted against time, shown in the upper graph in black. B) Time series of HONO and  $\text{HNO}_3$  from the 10 August to 11 August. Samples were taken at North Fork Idaho, 70 km north of the RFF. Of note are the enhancements of HONO during the nighttime hours, and enhancements of  $\text{HNO}_3$  during the daytime hours.

HONO concentrations ranged from 50–150 pptv throughout much of the afternoon of 10 August (Figure 9; blue) and  $\text{HNO}_3$  levels varied between 50–175 pptv (with a single spike reaching 231 pptv Figure 10; red). Ratios of HONO/ $\text{HNO}_3$  remained low, averaging around 0.6

(Figure 9A). By early evening,  $\text{HNO}_3$  began a slow decline reaching 10 pptv by next morning while HONO levels were variable and the ratio of  $\text{HONO}/\text{HNO}_3$  generally climbed from ~0.6 to 13, with oscillations following variation in HONO concentration.

### 3.1.2 12 – 13 August

On the drive from North Fork to Royal Gorge, the van passed through a visible smoke plume from the RFF between 10:40 and 12:35, with winds blowing from the South and plume age estimated at 1-2 hours (Figure 10C). HONO concentrations increased from 50 pptv to ~600 pptv in the first visibly thicker parcel of smoke impacted air, while the  $\text{HONO}/\text{HNO}_3$  ratio averaged 4.2 (Figures 10A and 10B). After passing into visibly clearer air the  $\text{HNO}_3$  and HONO levels remained relatively constant and the  $\text{HONO}/\text{HNO}_3$  ratio averaged 0.4 during afternoon stationary and mobile measurements. In the evening,  $\text{HNO}_3$  steadily decreased while HONO remained near 50 pptv.

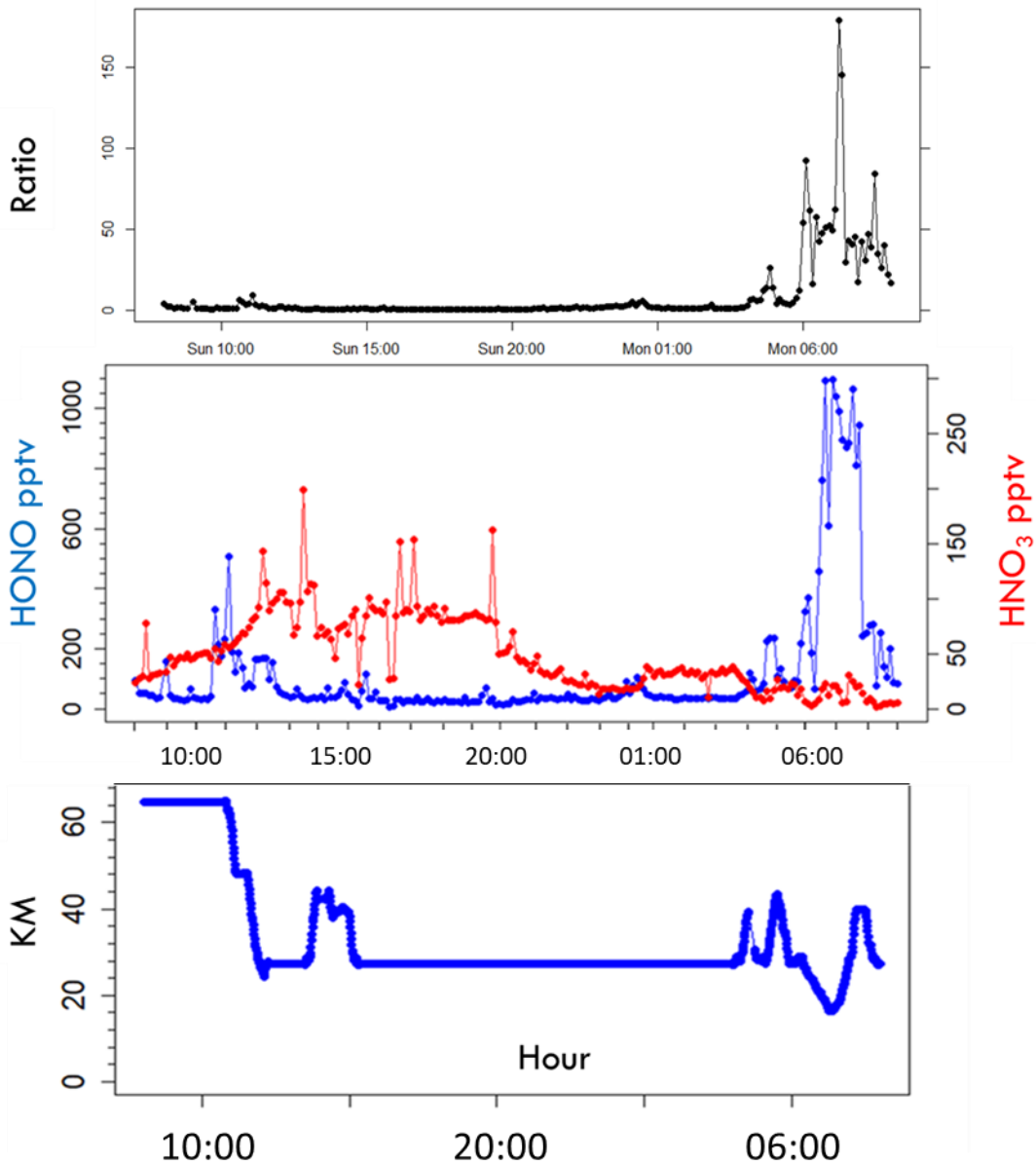


Figure 10: a) Ratio of HONO vs HNO<sub>3</sub> plotted vs time. b) Time series of HONO and HNO<sub>3</sub> on 12 August and 13 August. Note periods of enhanced HONO in the early morning hours of 13 August, in excess of 1000 pptv; as well as periods of enhanced HNO<sub>3</sub> in the afternoon of 12 August, with concentrations in excess of 100-150 pptv. Note that HONO and HNO<sub>3</sub> are plotted on different y-axis scales. c) Subset of Figure 8 showing the detailed distance from the RFF during the 12 August and 13 August.

At 04:00 on 13 August mobile measurements began on highway 93 between Ellis and Challis. We encountered thick smoke 20 minutes later near the intersection with MCR, marked by a HONO spike reaching 235 ppt and an average HONO/HNO<sub>3</sub> ratio of 18 (Figure 10). As the

van turned up MCR, there was a pulse of smoke and HONO increased to 368 pptv with an average HONO/HNO<sub>3</sub> ratio of 56. While the van never reached the barricade marking the area closed by the Forest Service, our team collected two samples estimated to be 7-10 km from the flame front of the RFF. The concentration of HONO was > 600 pptv from 06:35 – 07:50 and peaked at 1100 pptv, with HONO/HNO<sub>3</sub> ratios averaging 64. In the two samples collected when the van stopped at closest point to the RFF on this mobile run, the ratios were 165 and 145, with HONO concentrations at 893 and 870 pptv, respectively. The ratios in these two samples are the largest in the campaign, driven mainly by the low concentrations of HNO<sub>3</sub> (on the order of 50 pptv) rather than extreme levels of HONO. The nocturnal inversion lifted during this time, resulting in clearer air and more distinct and defined plume edges, as noted by the Forest Service in their twice daily updates.

### 3.1.3 13 – 14 August

After recalibration, the MC/IC conducted stationary sampling at Royal Gorge from 11:40 – 22:20 (Figure 11C). The wind came primarily from the East, bringing well-aged air masses likely impacted by the Goldstone Fire, ~ 40 km NE of Royal Gorge. HONO concentrations were ~100 pptv, HNO<sub>3</sub> levels increased from ~75 pptv to ~150 pptv, and the ratio of HONO/HNO<sub>3</sub> remained low, with an average of 0.46 (Figures 11A and 11B). At 18:46 HNO<sub>3</sub> levels began to steadily decrease to 50 pptv by 22:00, and HONO decreased from 50 to 20 pptv.

Mobile measurements began at 22:20, and upon pulling out of the shallow Royal Gorge valley, we were inundated with smoke, easily detectable by smell and visual haze (Figure 11C). Within forty minutes of leaving Royal Gorge, HONO concentrations rose to over 600 pptv, while HNO<sub>3</sub> concentrations remained under 100 pptv, and the HONO/HNO<sub>3</sub> ratio grew from 0.4 to 8

(Figures 11A and 11B). We drove up MCR and reached the forest service barricade at 23:26 and sampled for ~7 minutes. It is important to note that the Forest Service expanded the closure area around RFF during 13 August, moving the barricade 4 km further down the road than where the van had turned around early that morning. After the sample collection, we drove back to ID-93 south toward Challis and onto Challis Creek road and then returned to MCR by 02:00. During this drive, HONO remained elevated, albeit variable, and HONO/HNO<sub>3</sub> ratios fluctuated between 4 and 10, with two major jumps to 17 and 24. HNO<sub>3</sub> generally remained between 50–100 pptv. See Appendix A for a detailed description of this time period.

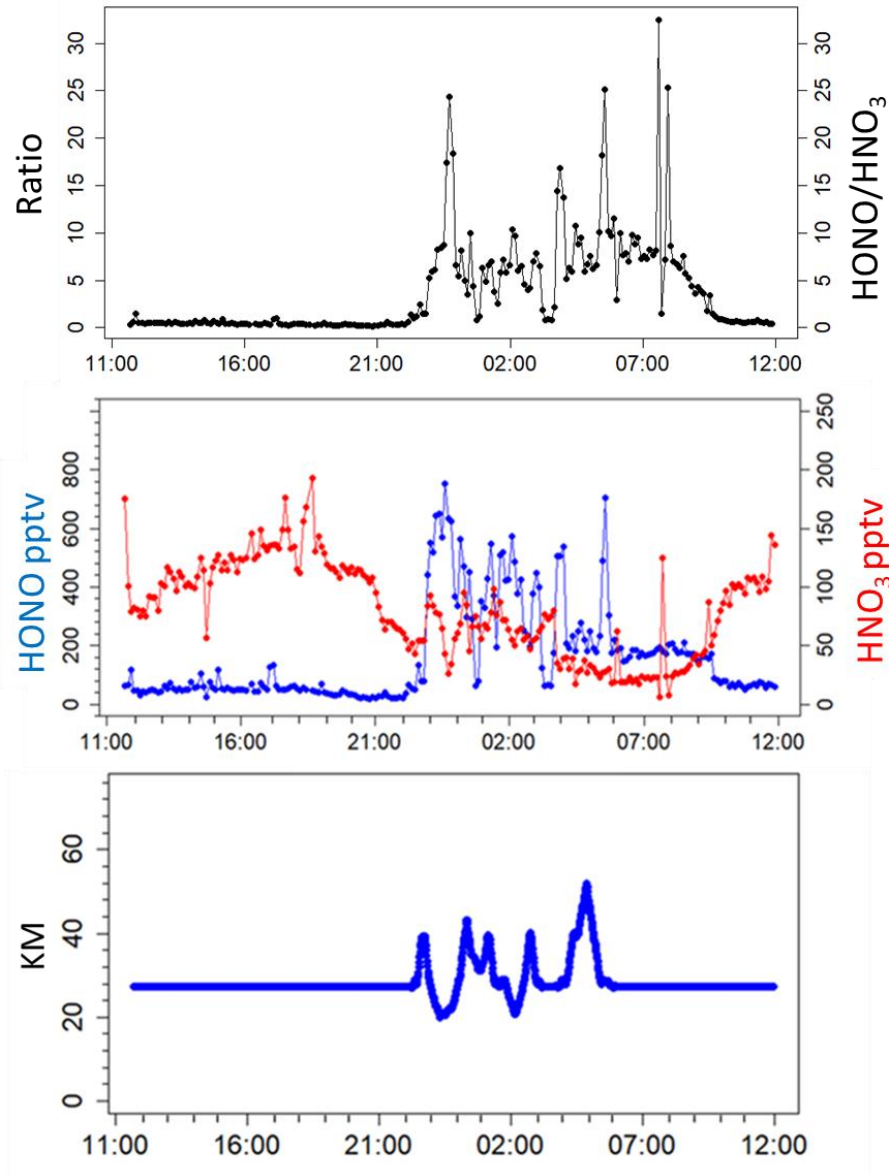


Figure 11: A) Ratio of HONO vs HNO<sub>3</sub> plotted vs time. B) Time series of HONO and HNO<sub>3</sub> on 13 August and 14 August. Note periods of enhanced HNO<sub>3</sub> during the afternoon of the 13th, that slowly decline. HONO is enhanced in the early morning hours of 14 August, coupled with periods of enhanced HNO<sub>3</sub>. Note that HONO and HNO<sub>3</sub> are plotted on different y-axis scales. C) Subset of figure 8 showing the more detailed distance from the RFF during 13 August and 14 August

At 02:50 we descended MCR again and headed back towards Royal Gorge for a driver change, where HONO levels went down dramatically, to 65 pptv, and HNO<sub>3</sub> levels rose to 77 pptv, driving the ratio down to 0.8. After 03:40, the second team made measurements between Royal Gorge and Challis for two hours, measuring HONO between 150 and 230 pptv, HNO<sub>3</sub>

between 25 and 30 pptv, and HONO/HNO<sub>3</sub> ratios between 6 and 10. A major HONO spike was observed at 05:34 as the van was driving North towards Royal Gorge from Challis and intercepted an air parcel of 'fresh smoke', somewhat aged, being blown SW from the RFF. It is important to note the high variability in the HONO and HNO<sub>3</sub> concentrations during this period of sampling. Increases and decreases in the two species are sometimes in phase and sometimes out of phase with one another. Based on Forest Service reports there was strong inversion layer present this night that trapped the smoke in the valley, blurring the edges of individual plumes and increasing the variability of the concentrations of the two species. Upon returning to Royal Gorge at 06:00, we made stationary measurements for the remainder of the morning. At 09:30 HONO dropped below 100 pptv and HNO<sub>3</sub> began a steady rise to 140 pptv, resulting in the drop of HONO/HNO<sub>3</sub> ratios from 7.5 to 0.45.

#### 3.1.4 14 -15 August

On 14 August the RFF grew 7,000 acres, from 16,000 acres to 23,000 acres; one of the largest days of growth for the fire, with most of the growth occurring on the upper NE side of the fire, and smaller growth happening on the southern end, close to the Spike Camp. A smoke impacted air mass was intercepted on the afternoon of 14 August while the van was stationary at Royal Gorge, with one small excursion north resulting in a dip in both HONO and HNO<sub>3</sub> (Figure 12). While at Royal Gorge, the air mass blew from the NE and was moderately aged. HONO concentrations reached up to 323 pptv and HNO<sub>3</sub> increased slightly from 270 pptv to 338 pptv and HNO<sub>3</sub> peaked at 488 pptv. The HONO/HNO<sub>3</sub> ratio stayed relatively constant between 0.32-1.0. Once the impacted air mass passed over Royal Gorge, HONO levels stabilized between 20 and 40 pptv, and HNO<sub>3</sub> levels slowly decreased to 50 pptv.

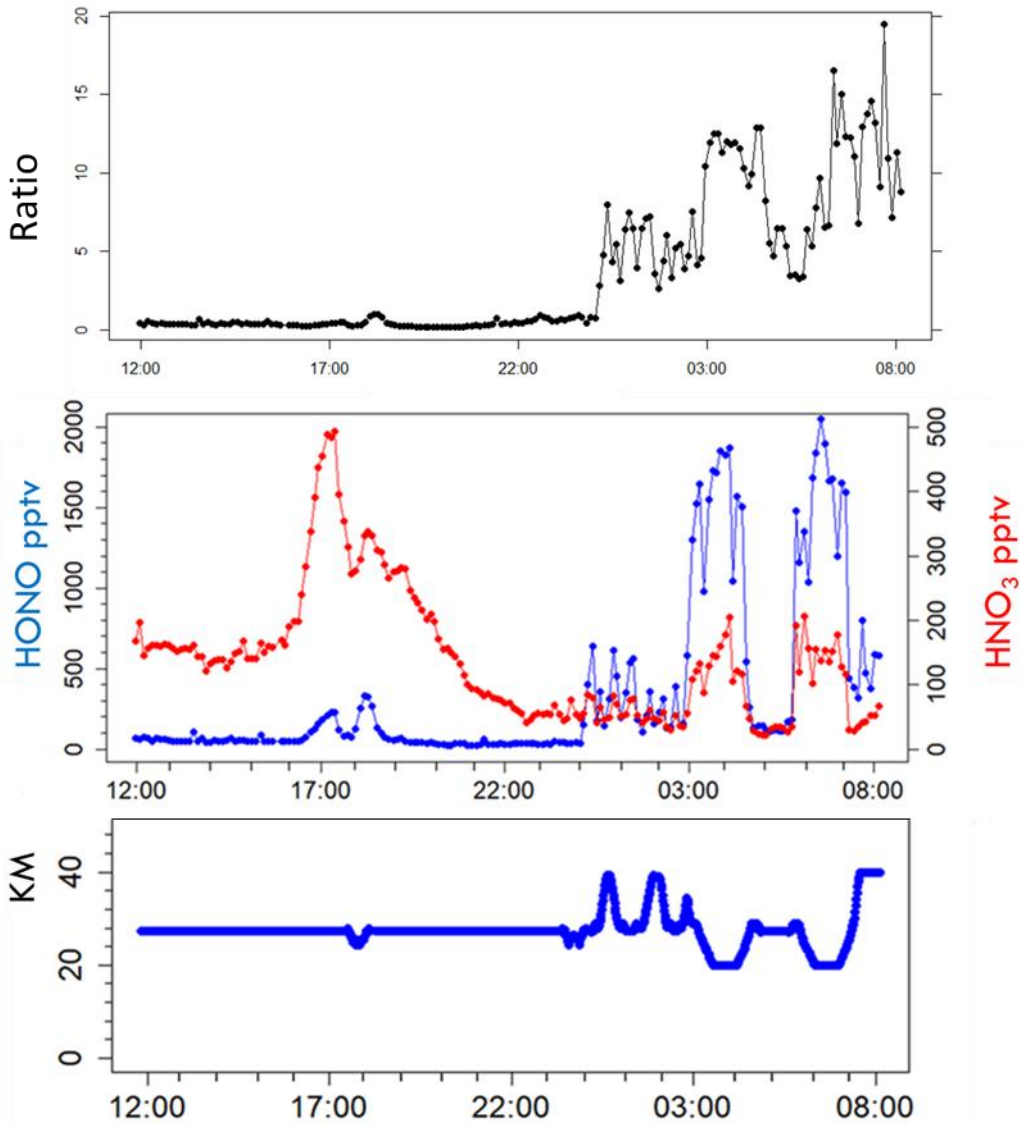


Figure 12: A) Ratio of HONO vs HNO<sub>3</sub> plotted vs time. B) Time series of HONO and HNO<sub>3</sub> from 12:00 on 14 August to 08:00 on 15 August. Of note are the enhancements of HONO and HNO<sub>3</sub> that correspond with differing magnitude during day and night time hours. HONO and HNO<sub>3</sub> are plotted on different y-axis scales. C) Subset of Figure 8 showing the more detailed distance from the RFF during 14 August and 15 August.

Mobile measurements began at 23:22, encountering smoke as the van passed the junction of MCR and ID-93 (Figure 12C). Five passes were made across the MCR/93 junction from the start of mobile measurements until 02:22 on 15 August. These passes are marked by HONO enhancements up to 693, 613, 562, and 392 pptv, respectively, from a baseline near 35 pptv (Figure 12B). HNO<sub>3</sub> levels showed the same trend, spiking in phase with the HONO spikes, 30-

50 pptv on top of a 30 pptv baseline. The HONO/ HNO<sub>3</sub> ratio in the MC drainage increased to 7.9, 7.4, 7.2, 5.9, 5.4, and 7.5 in the successive crossings, above a baseline averaging 4.7 (Figure 13A). After making the passes by the mouth of MCR, we turned up the road and drove to the barricade (02:20- 03:30) and made stationary measurements until 04:10, before returning to Royal Gorge for a driver exchange. During the drive up MCR, HONO generally increased, peaking at 1650 ppt, but oscillated between samples by several hundred pptv. Nitric acid covaried with HONO, peaking at 132 pptv with proportionately smaller variations between samples. At the barricade HONO ranged 1547 – 1873 pptv and HNO<sub>3</sub> ranged 129 – 204 ppt. During the entire period the van was on MCR the HONO/HNO<sub>3</sub> ratio ranged 8.2 – 12.5 (average 11.5), with no obvious enhancement during the stationary sampling at the barricade. After we exchanged drivers, the new crew returned to the barricade up MCR from 05:46 to 07:34. During this time we saw similar enhancements in HONO (2052 pptv) and HNO<sub>3</sub> (177 pptv). However, these enhancements occurred out of phase, with HNO<sub>3</sub> peaking twenty minutes after HONO. The HONO/HNO<sub>3</sub> ratio varied between 6 and 14.

### 3.1.5 15 – 16 August

Mobile measurements were made between Salmon and Royal Gorge during the afternoon of 15 August, hoping to intercept a scheduled flyover by the WE-CAN C-130 (Figure 13C). The drive from Royal Gorge to Salmon was characterized by fluctuating HONO levels between 60 – 160 and equally variable changes in HNO<sub>3</sub> concentrations, between 128-286 pptv (Figure 13B). The spikes in concentration for the two species were out of phase and the HONO/HNO<sub>3</sub> ratio varied between 1.5 and 5 (Figure 13A). The wind was sweeping the smoke directly across ID-93, blowing from the SW, from the RFF. Once in Salmon the van remained stationary (13:06 to 13:42), marked by equally variable concentrations in both HONO and HNO<sub>3</sub>. At 13:50 the van

began the drive to Challis, observing large HONO enhancements, peaking at 458 pptv, with HNO<sub>3</sub> peaking at 250 pptv, seven minutes before the HONO spike. HONO/HNO<sub>3</sub> ratios peaked at 2 and averaged around 1.

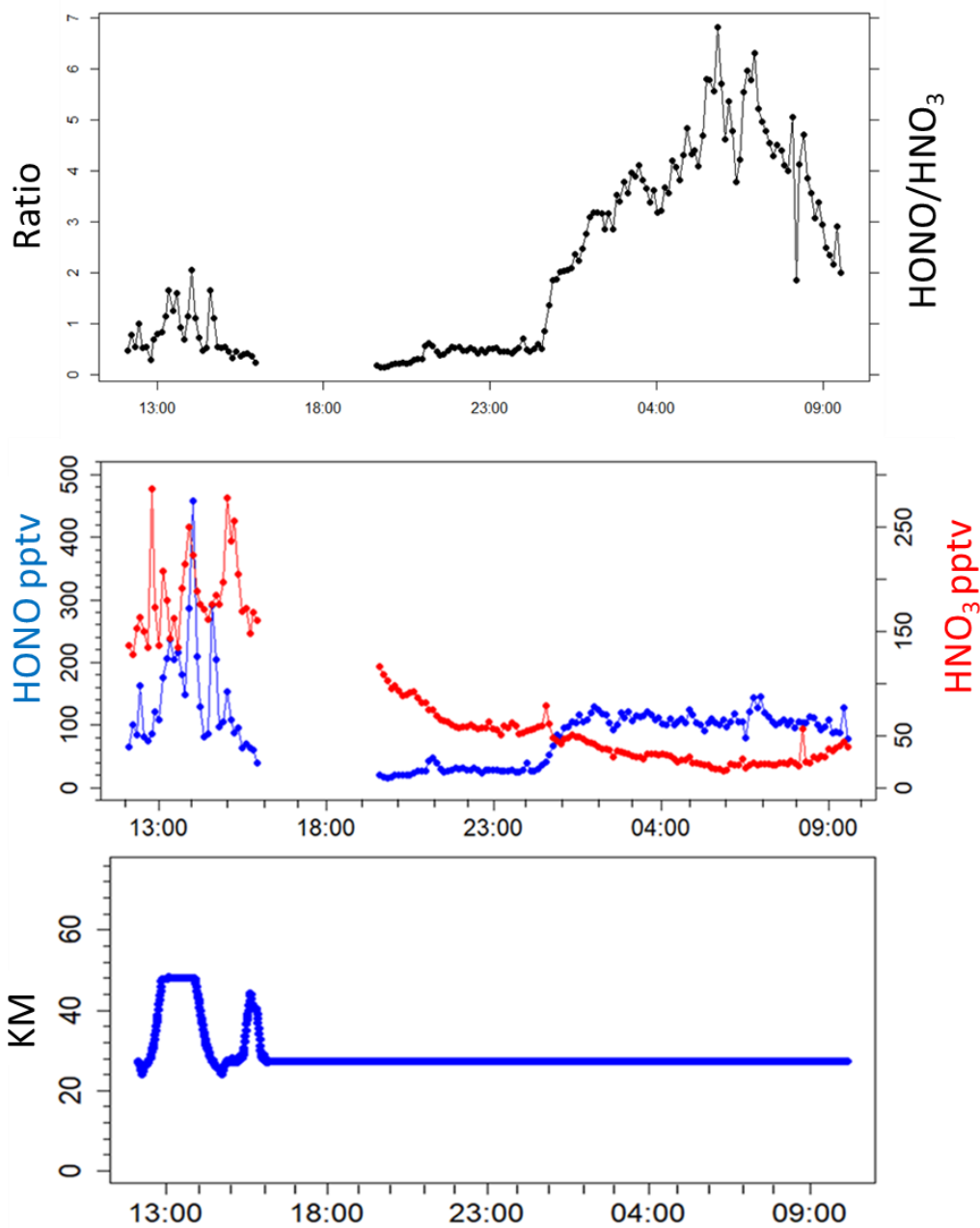


Figure 13: A) Time series including dilute smoke sampling on 15 August and 16 August. Measurements were made between Salmon and Royal Gorge. Note the diurnal differences between HONO and HNO<sub>3</sub>. HONO and HNO<sub>3</sub> have been plotted on different y-axis scales. B) Subset of Figure 8 showing the more detailed distance from the RFF during 15 August and 16 August.

Stationary measurements at Royal Gorge from the evening of 15 August and into the morning of 16 August showed low HONO levels between 16 pptv and 26 pptv while HNO<sub>3</sub> concentrations slowly declined from 116 pptv to 42 pptv. The ratio of the two species slowly increased from 0.1 to 0.9. Around midnight, HONO levels suddenly increase from 26 pptv to 130 pptv, while HNO<sub>3</sub> slowly decreases to a low of 17 pptv, and the HONO/HNO<sub>3</sub> ratio increased from 0.9 to 6. At 08:00 HONO levels begin to fall, and HNO<sub>3</sub> levels start to increase. The ratio of the two species fell from 6 to 2.

### 3.1.6 Daytime Spike Camp Measurements on 16 August

On 16 August, daytime measurements were made in fresh smoke at Spike Camp, past the barricade on MCR where we had previously been sampling (Figure 14). This was the closest approach to the RFF we were able to achieve, at 10.7 km from the fire start and 2 km from the fire line. At 14:56 we left Royal Gorge and drove to MCR arriving at Spike Camp at 16:02 (Figure 14C). During the drive to Spike Camp the air we were sampling decreased drastically in age (from well-aged to very young). This shift occurred as we drove up MCR into fresher air parcels as we gained in elevation. The prevailing winds blew from the N/NE, from the RFF directly towards Spike Camp. As we approached Spike Camp HONO concentrations became more variable, fluctuating between 60 and 180 pptv and HNO<sub>3</sub> concentrations decreased from 150 pptv to 60 pptv (Figure 15B). The ratio of HONO/HNO<sub>3</sub> stayed between 0.5-1 for the duration of the climb, varying with the spikes and dips in HONO concentration (Figure 14A).

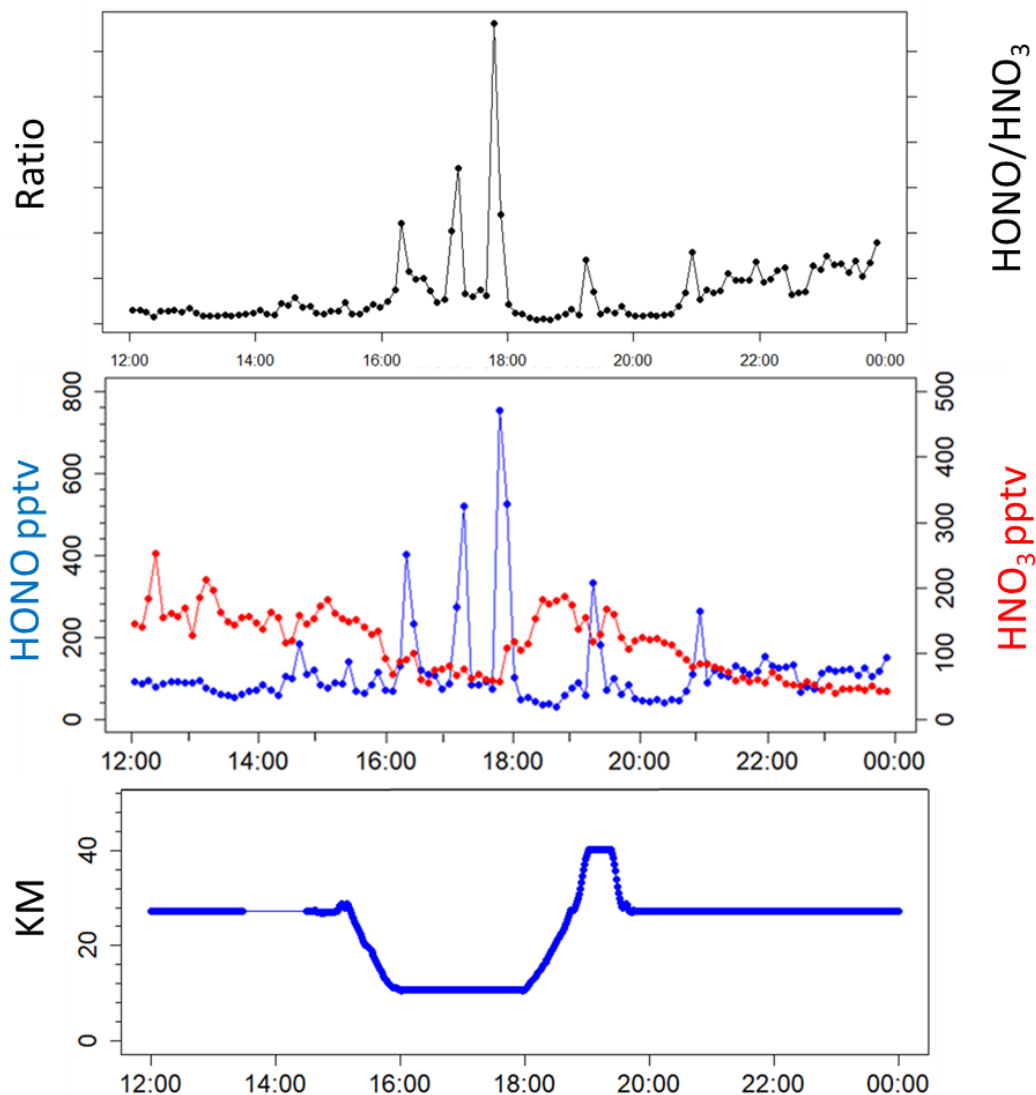


Figure 14: Time series of daytime sampling on 16 August including samples taken at Spike Camp. Note the three large daytime spikes of HONO and decreasing HNO<sub>3</sub> in the fresh smoke as compared to the more aged smoke.

While we were stationary at Spike Camp, from 15:57 pm – 18:00 pm, 3 different puffs of smoke mixed down to the van, visualized by the spikes in HONO concentrations. These spikes reached 400, 519, and 725 pptv of HONO. Corresponding HNO<sub>3</sub> concentrations were 91, 76, and 57 pptv, and generally represented decreases in the HNO<sub>3</sub> concentration. The HONO/HNO<sub>3</sub> ratio in the successive puffs of thick smoke were 4, 6.8, and 13, compared to 1.5 during the rest of

stationary sampling at Spike Camp. As we began our descent down MCR and back into more aged smoke, the  $\text{HNO}_3$  concentrations rose back to daytime levels between 120 and 180 pptv, and HONO decreased to below 100 pptv, and even below 50 pptv for several consecutive samples. The HONO/ $\text{HNO}_3$  ratio decreased to 0.2-0.4. At 19:08 we encountered a BB impacted air mass on ID-93 as we drove towards Royal Gorge. HONO spiked to 332 pptv for one sample, while  $\text{HNO}_3$  dropped from 170 pptv to 118 pptv. We returned to Royal Gorge at 19:39 and measured a smaller HONO spike of 264 pptv and corresponding drop in  $\text{HNO}_3$  levels from 120 pptv to 80 pptv. Both small HONO spikes occur in young air masses, separated by air that was much more aged. Between 20:00 and 22:00 hours,  $\text{HNO}_3$  decreased to night levels around 50 pptv while HONO levels began to slowly build.

#### CHAPTER 4: DISCUSSION

During the period of mobile measurements taken on the morning of 13 August on MCR (Figure 11), we observed the highest ratio of HONO/ $\text{HNO}_3$  seen the entire campaign. The ratio averaged 64.4 and peaked at 165 and 147 in two consecutive samples. These samples were taken between 7-10 km from the RFF. We believe that the variation in these samples is driven in part by the variability of the environmental conditions. Wind speed and direction differ in and out of valleys, influenced by the rapidly changing terrain. The drive between ID-93 and the barricade is characterized by a change in environment from flat valleys between mountains, to the narrow passes in the mountains. The peak ratios measured on 13 August do not correspond to times of peak HONO concentrations measured on the same night. HONO concentrations roughly 20% higher were measured just before and just after the peak ratios. The exceptionally high HONO/ $\text{HNO}_3$  resulted from depressed  $\text{HNO}_3$  concentrations (just 5 and 6 pptv, respectively). In thicker smoke (indicated by higher HONO concentrations) sampled before and after the peak

ratios,  $\text{HNO}_3$  was 4 – 5 times more abundant but still depressed compared to other days when the van was on MCR.

It would have been useful to have a conservative tracer, such as CO, to constrain dilution of measured airmasses during all mobile sampling. Unfortunately, we were not able to operate the LGR and Piccaro instruments during mobile measurements due to power limitations. We note that the peak HONO/ $\text{HNO}_3$  ratios measured on 13 August (Figure 11) are comparable to HONO/ $\text{HNO}_3$  emission ratios measured in the 2016 FIREX lab experiments (Figure 15) (Chai et al., 2019). Based on the 2016 FIREX lab experiments, we can confidently assume that HONO is a primary emission while  $\text{HNO}_3$  is predominantly produced as the smoke is chemically processed. In the 24 stack burns sampled during the Fire Lab experiment, the HONO/ $\text{HNO}_3$  ratio was  $> 36$  in all but two smoldering fires burning duff (mean 178, standard deviation 165) (Figure 15 A, and Chai et al., 2019).

The measurements of the RFF on the morning of 13 August also reflect trends from the FIREX lab experiments, where Figure 10 B shows high HONO/ $\text{HNO}_3$  ratios as a clear indicator of “fresh” smoke, with ratios starting very high,  $\sim 80$ , and decreasing as the smoke ages, to  $< 10$ . The ratios of HONO/ $\text{HNO}_3$  measured on the morning of 13 August as we were ascending and descending MCR, before we began measurements at the barricade, were lower than the peak ratios, averaging around 58. We therefore assume that the smoke measured during the two peak ratios was the freshest, least processed smoke sampled during the campaign, punctuated by slightly older more processed smoke. In the older smoke surrounding these peak ratios, we see that  $\text{HNO}_3$  is building up more rapidly than HONO is being produced, driving down the ratio of the two species as the plume ages. This rapid net production of  $\text{HNO}_3$  during nighttime hours, seen here and on other nights, is unexpected, and not documented in literature up to this point.

We suggest that this behavior provides evidence of net production of  $\text{HNO}_3$  at night in the absence of photochemistry.

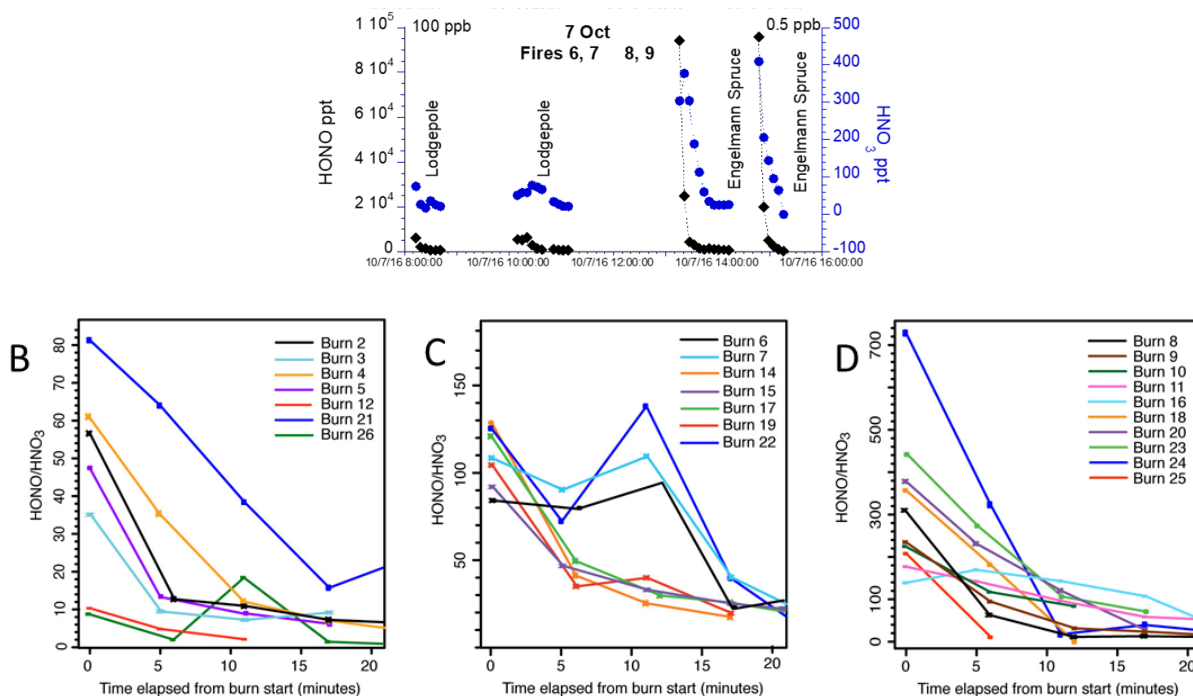


Figure 15: A) Emission of HONO and  $\text{HNO}_3$  for burns 6-9 during FIREX 2016. Note the two species are plotted on different y-axis scales. B/C/D) HONO/ $\text{HNO}_3$  ratio for FIREX burns 2-12; 14-26 displaying the high ratio at the onset of combustion, as well as the declining ratio as the burns continued. Burns are binned by magnitude of the ratio. For more information on burns, including composition, see Semilovic et al., (2018).

The night of 13 August highlights how the ratio of HONO/ $\text{HNO}_3$  is a useful metric for determining a relative plume age (or degree of smoke processing). Figure 11A shows that ratios of HONO/ $\text{HNO}_3$  near the MCR barricade (16-24) were sometimes twice as large as ratios seen just 5 minutes down the road (6-8). We theorize that this change in ratio is driven by a higher net production of  $\text{HNO}_3$  than HONO as the plume ages and processes combined with the slow movement of the plume. However, Figure 11 also demonstrates how variable the same plume can be within the span of a few hours to a few minutes. From sample to sample there can be up

to a 50% difference in concentration (Figure 11B). Concentrations of HONO and HNO<sub>3</sub> during that mobile sampling interval varied dramatically from one sample to the next, with a  $\Delta$ HONO as large as 400-500 pptv in consecutive 5-minute samples. These variations on short time scales likely reflect complicated transport and vertical mixing processes as opposed to rapid chemistry. Despite the noise in the measurements, we see strong evidence for evolution of the smoke chemistry by the relative increase in HNO<sub>3</sub> as compared to HONO.

While ratios of HONO/HNO<sub>3</sub> seen during WE-CAN 2018 are lower than those seen during the FIREX Fire Lab experiments, we still see particularly high ratios on the morning of 13 August, as compared to other days. The fact that the ratio decreases with “aging” even during the night suggests that net production of HNO<sub>3</sub> is occurring much faster than any secondary production of HONO. Smoke sampled during the day had even lower HONO/HNO<sub>3</sub> ratios. Part of this discrepancy could be due to continued production of both acids at different rates, but the loss of HONO by photolysis is also contributing to the lower daytime ratios. It again would be useful to have CO to use as a tracer to inform the level dilution of the plumes allowing a better comparison of rates of secondary production of HONO and HNO<sub>3</sub>. Throughout this campaign, in the absence of a conserved tracer, the variations in HONO concentrations served as our main marker of smoke impacted air. We can assume that intervals with sharp increases in HONO concentrations, and high variability from sample to sample, are indicative of smoke impacted air masses. This does not mean, however, that this method is ideal. The variation in HONO throughout plumes makes it hard to interpret quantitative changes in the plume without a conservative tracer like CO. While HONO is a good indicator of when we are in the plumes and can give a rough estimate of how dense the smoke is, we are unable to constrain the extent of dilution without a conservative tracer.

With the knowledge that highly variable HONO concentrations are indicative of smoke impacted air masses, we can then assume that intervals with smoothly varying HONO concentrations reflect the sampling of background, or ambient air. These smooth transitions were seen in the nighttime intervals on 12–13 August and 15–16 August. On the night of 12 August, HONO concentrations started at 35 pptv at 20:00, and remained between 20-35 pptv until midnight. HONO then crept up to 50-60 pptv, before it returned to levels ~35 pptv at 01:00 (Figure 11). HONO concentrations remained steady ~35 pptv until 04:00 when mobile measurements were started. The night of 15 August showed similar smooth trends in HONO and HNO<sub>3</sub>. Starting at 20:00 HONO was low, ~20-30 pptv until midnight, where it increased to between 100-120 pptv. HONO stayed around that level until just after 09:00 where it rapidly dropped back down to levels ~30 pptv. Each of these transitions are marked by very little difference from sample to sample, unlike the highly variable behavior seen in impacted airmasses.

While HONO is photochemically degraded during the day, in “fresh” smoke during daytime hours enhanced levels are still measured, as seen on the afternoon of 15 August (Figure 13), and during the daytime Spike Camp measurements on 16 August (Figure 14). In these examples the air sampled moderately aged and fresh, respectively. Both cases occur in daylight and show elevated HONO despite being highly photochemically reactive. HONO levels spike at ~500 pptv on 15 August during mobile measurements between Salmon and Challis. The RFF grew substantially that day on the NE side with winds blowing emissions from the SW, towards the mobile lab as we sampled up and down ID-93. HNO<sub>3</sub> levels at this same time are elevated to ~250 pptv, highly indicative of more aged smoke that has had time to process. The measurements taken at Spike Camp on 16 August also reveal this daytime HONO enhancement

despite photolytic destruction. The smoke sampled at very close proximity to the RFF on this day shows HONO levels upwards of 800 pptv, and corresponding decreases in HNO<sub>3</sub> concentration. This pattern is representative of extremely fresh smoke. The ratio for HONO/HNO<sub>3</sub> while sampling at Spike Camp is around 0.2-0.5 outside of the HONO spikes. Within the three major HONO spikes the ratio jumps to 4, 4, and 13 respectively, which are much lower than seen in the Fire Lab experiments, or most night time sampling in thick smoke during this campaign, but higher than HONO/HNO<sub>3</sub> ratios in ambient air.

In the early morning hours of each day that we sampled smoke impacted plumes, there was an increase in the ratio of HONO/HNO<sub>3</sub> to 10 and sometimes above. This ratio persists, along with the observed HONO concentrations, into the early morning hours, past sunrise, consistent with Nie et al. (2015). Around 08:00 hours the ratio drops to ~1, as HONO is broken down by photolysis and HNO<sub>3</sub> builds up through secondary production. During the day the ratio of the two species remains below 1 except in thicker smoke that occasionally mixed down to the surface until the early morning hours, where it once again spikes to 10 or above, before the net production of HNO<sub>3</sub> overtakes that of HONO and drives the ratio back down.

Figure 16 compares mean HONO/HNO<sub>3</sub> ratios for smoke-impacted (HONO > 50 pptv) and background (HONO < 50 pptv) airmasses. By defining a baseline (green boxes) we can clearly see that smoke impacted air masses (grey boxes) have significantly different HONO/HNO<sub>3</sub> ratios than ambient air masses, with a diurnal variation apparent in both types of airmasses. Using HONO/HNO<sub>3</sub> ratios as a signature for smoke is much more noticeable at night when HONO has a longer lifetime.

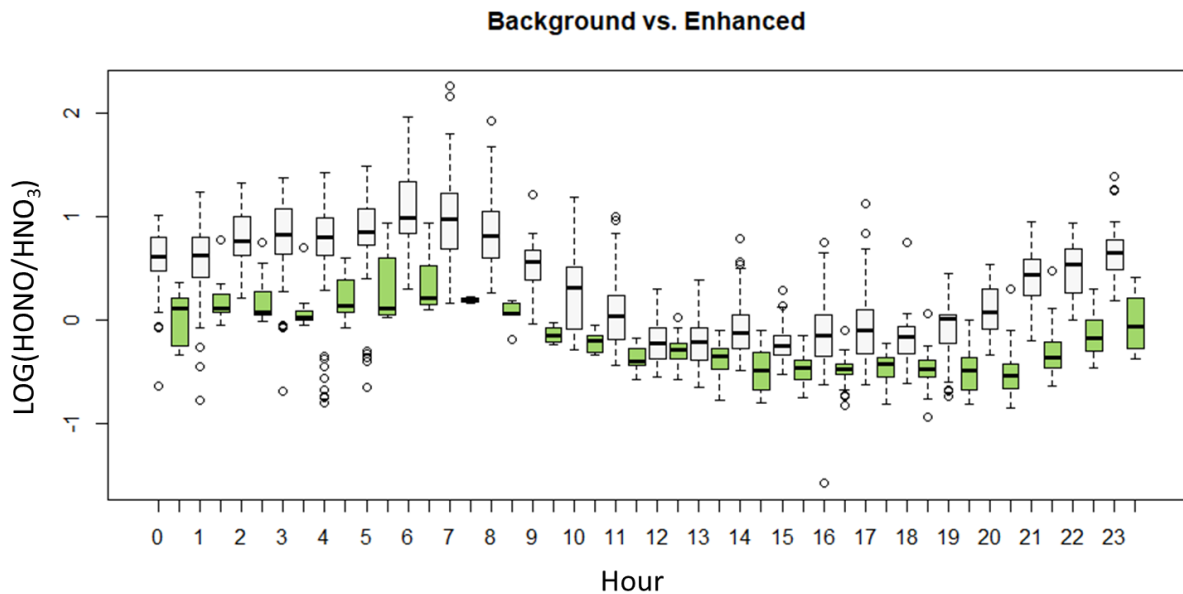


Figure 16: Plot of  $HONO/HNO_3$  binned by hour and background (<50 pptv, green) vs enhanced (>50 pptv, grey)  $HONO$  concentrations. This reveals that there is an ambient level of  $HNO_3$  that needs to be taken into consideration when qualifying if air masses are smoke impacted. The plot reflects the impacts of smoke that we see at night as compared to the smaller, but still significant perturbation in the daytime hours. Note the boxes contain middle 50% of data, top and bottom whiskers contain the top and bottom 25% of data, and points above and below the whiskers denote outliers in the dataset.

Based on the successes of the 2018 WE-CAN campaign, we recommend continuing several approaches for successful monitoring of smoke impacted air masses. Communication with the local Forest Service branches was an invaluable resource. They were able to recommend areas that were heavily impacted by smoke and that would be accessible to our van. They also provided detailed maps of the fire growth for each successive day, and information regarding the movements of the firefighters based on their perception of the local air quality. Communication with the Forest Service was the sole reason we were able to gain access to the Spike Camp to measure close to the fire (within 2 km of the fireline). The Forest Service was interested in our research as it pertained to air quality and monitoring the health of their firefighters. They extended a gracious helping hand to us for the duration of our campaign. The discovery of MCR

was another valuable contribution to our campaign. We were able to approach the fire under a multitude of different conditions, with confidence that we would intercept an impacted air mass. Identifying and utilizing a road allowing similar access to a fire would be an asset to future campaigns.

Moving forward into the 2019 FIREX Campaign, we also advise the following improvements in data collection. Primarily, there is a need for a conservative tracer such as CO, as stated previously. The addition of a conservative tracer to our data would have allowed us to determine with more accuracy and certainty the dilution and relative age of the air masses sampled. An accurate real time indicator of air mass age, such as NO<sub>x</sub>, would have been an additional boon to our measurements. With this information we would have been able to determine if we were in smoke impacted air masses with more accuracy than sight and smell.

## CHAPTER 5: CONCLUSIONS

Our understanding of smoke plume chemistry in wildfires is still new and continuously evolving. A multitude of variables influence our ability to capture the intricacies of smoke plume chemistry, including wind speed and direction, physical access to plumes, and proximity to plumes. Terrain plays an important role in the movement of air masses and therefore accessibility of smoke plumes. Valleys tend to funnel smoke downhill if they are in close enough proximity to a fire, as seen in our multiple passes by MCR. However, ridges and atmospheric inversions can also prevent the smoke impacted air masses from entering a valley if they are located further away from the fire front, preventing successful sampling of wildfire plumes.

Daytime lofting of airmasses often limited our access to the plumes, and we only saw the small perturbations of the plumes that made their way down to the surface. While these perturbations were likely not representative of the plumes in total, they were more heavily impacting local surface air quality than the plumes that never reached the ground. Although our ground-based measurements might not have been able to characterize the overall smoke plumes, they did provide important information about plume chemistry and composition on and near the surface on a local scale.

Within the plumes we measured, high sample to sample variability in HONO and HNO<sub>3</sub> was our best indicator that we were measuring smoke impacted plumes in the absence of a conservative tracer. Using meteorological data as well as the recorded location of our van, we confirmed the time in which we measured impacted air masses. Within these intervals, HONO and HNO<sub>3</sub> varied as much as 50% from sample to sample. In contrast, measurements made in ambient air were markedly different, with very little change in species concentrations from sample to sample.

The measurements and observations from this study have furthered our understanding of reactive nitrogen chemistry in smoke impacted air masses. In our measurements the ratio of HONO to HNO<sub>3</sub> presented a distinct signature of impacted versus background air during the day and night. Ratios in plumes sampled during the day generally stayed low and went even lower in airmasses not impacted by smoke. Ratios indicative of freshly impacted air masses during the night frequently showed ratios at 10 and above, and in one case approached 150, within the range of measurements made in the Fire Lab during FIREX 2016. Daytime plumes showed a more modest enhancement of HONO/HNO<sub>3</sub>, in the range of 4-6. Importantly, the nighttime ratios of HONO to HNO<sub>3</sub> persisted into daytime hours and daytime ratios persisted into the early evening,

indicating a delay in chemical processing within the plumes. In addition, our measurements reveal a net production of  $\text{HNO}_3$  that outweighs HONO production during both the daytime and nighttime regimes.

## BIBLIOGRAPHY

- Akagi, S. K., Craven, J. S., Taylor, J. W., Mcmeeking, G. R., Yokelson, R. J., Burling, I. R., et al Weise, D. R. (2012). Evolution of trace gases and particles emitted by a chaparral fire in California. *Atmos. Chem. Phys. Atmospheric Chemistry and Physics*, *12*, 1397–1421. <https://doi.org/10.5194/acp-12-1397-2012>
- Akagi, S. K., Yokelson, R. J., Wiedinmyer, C., Alvarado, M. J., Reid, J. S., Karl, T., et al Wennberg, P. O. (2011). Emission factors for open and domestic biomass burning for use in atmospheric models. *Atmos. Chem. Phys. Atmospheric Chemistry and Physics*, *11*, 4039–4072. <https://doi.org/10.5194/acp-11-4039-2011>
- Benedict, K. B., Prenni, A. J., Carrico, C. M., Sullivan, A. P., Schichtel, B. A., Collett, J. L., et al Collett, J. L. (2017). Enhanced concentrations of reactive nitrogen species in wildfire smoke. *Atmospheric Environment*, (15), 8–15. <https://doi.org/10.1016/J.ATMOSENV.2016.10.030>
- Blaisdell, R., & Lipsett, M. (2001). Wildfire Smoke A Guide for Public Health Officials. Retrieved from <https://www3.epa.gov/ttnamti1/files/ambient/smoke/wildgd.pdf>
- Bytnerowicz, A., Hsu, Y.-M., Percy, K., Legge, A., Fenn, M. E., Schilling, S., et al Alexander, D. (2016). Ground-level air pollution changes during a boreal wildland mega-fire. *Science of The Total Environment*, *572*, 755–769. <https://doi.org/10.1016/J.SCITOTENV.2016.07.052>
- Chai, J., Miller, D., Scheuer, E., Yokelson, R., Brown, S., Dibb, J., & Hastings, M. (2019) Isotopic characterization of nitrogen oxides, nitrous acid, and nitrate from laboratory biomass burning during FIREX, in Review with Atmospheric Measurement Techniques
- Coggon, M. M., Veres, P. R., Yuan, B., Koss, A., Warneke, C., Gilman, J. B., ... de Gouw, J. A. (2016). Emissions of nitrogen-containing organic compounds from the burning of herbaceous and arboraceous biomass: Fuel composition dependence and the variability of commonly used nitrile tracers. *Geophysical Research Letters*, *43*(18), 9903–9912. <https://doi.org/10.1002/2016GL070562>
- Heck, W. W., Adams, R. M., Cure, W. W., Heagle, A. S., Heggestad, H. E., Kohut, R. J., et al Taylor, O. C. (1983). A reassessment of crop loss from ozone. *Environmental Science & Technology*, *17*(12), 572A-581A. <https://doi.org/10.1021/es00118a716>

- Jaffe, D. A., & Wigder, N. L. (2012). Ozone production from wildfires: A critical review. *Atmospheric Environment*, *51*, 1–10. <https://doi.org/10.1016/J.ATMOSENV.2011.11.063>
- Keene, W. C., Talbot, R. W., Andreae, M. O., Beecher, K., Berresheim, H., Castro, M., et al Winiwarter, W. (1989). An intercomparison of measurement systems for vapor and particulate phase concentrations of formic and acetic acids. *Journal of Geophysical Research*, *94*(D5), 6457. <https://doi.org/10.1029/JD094iD05p06457>
- Lin, J. C., Mitchell, L., Crosman, E., Mendoza, D. L., Buchert, M., Bares, R., et al Ehleringer, J. (2018). CO<sub>2</sub> and Carbon Emissions from Cities: Linkages to Air Quality, Socioeconomic Activity, and Stakeholders in the Salt Lake City Urban Area. *Bulletin of the American Meteorological Society*, *99*(11), 2325–2339. <https://doi.org/10.1175/BAMS-D-17-0037.1>
- Miller, D. J., Wojtal, P. K., Clark, S. C., & Hastings, M. G. (2017). Vehicle NO<sub>x</sub> emission plume isotopic signatures: Spatial variability across the eastern United States. *Journal of Geophysical Research: Atmospheres*, *122*(8), 4698–4717. <https://doi.org/10.1002/2016JD025877>
- Nie, W., Ding, A. J., Xie, Y. N., Xu, Z., Mao, H., Kerminen, V.-M., et al Fu, C. B. (2015). Influence of biomass burning plumes on HONO chemistry in eastern China. *Atmospheric Chemistry and Physics*, *15*(3), 1147–1159. <https://doi.org/10.5194/acp-15-1147-2015>
- Palm, B. B., Campuzano-Jost, P., Day, D. A., Ortega, A. M., Fry, J. L., Brown, S. S., et al Jimenez, J. L. (2017). Secondary organic aerosol formation from in situ OH, O<sub>3</sub>, and NO<sub>3</sub>; oxidation of ambient forest air in an oxidation flow reactor. *Atmospheric Chemistry and Physics*, *17*(8), 5331–5354. <https://doi.org/10.5194/acp-17-5331-2017>
- Ren, X., van Duin, D., Cazorla, M., Chen, S., Mao, J., Zhang, L., et al Kelley, P. (2013). Atmospheric oxidation chemistry and ozone production: Results from SHARP 2009 in Houston, Texas. *Journal of Geophysical Research: Atmospheres*, *118*(11), 5770–5780. <https://doi.org/10.1002/jgrd.50342>
- Salmon-Challis National Forest - About the Forest. (n.d.). Retrieved April 9, 2019, from <https://www.fs.usda.gov/main/scnf/about-forest>

Salmon-Challis National Forest - Fire Management. (n.d.). Retrieved April 18, 2019, from <https://www.fs.usda.gov/main/scnf/fire>

Salmon-Challis National Forest - Home. (n.d.). Retrieved April 18, 2019, from <https://www.fs.usda.gov/main/scnf/home>

Salmon-Challis National Forest - National Forest Foundation. (n.d.). Retrieved April 9, 2019, from <https://www.nationalforests.org/our-forests/find-a-forest/salmon-challis-national-forest>

Selimovic, V., Yokelson, R. J., Warneke, C., Roberts, J. M., De Gouw, J., Reardon, J., & Griffith, D. W. T. (2018). Aerosol optical properties and trace gas emissions by PAX and OP-FTIR for laboratory-simulated western US wildfires during FIREX. *Atmos. Chem. Phys*, 18(18), 2929–2948. <https://doi.org/10.5194/acp-18-2929-2018>

Statement of Work. (n.d.). FIREX Grant Submission 2016.

Talbot, R. W., Vijgen, A. S., & Harriss, R. C. (1990). Measuring tropospheric HNO<sub>3</sub>: Problems and prospects for nylon filter and mist chamber techniques. *Journal of Geophysical Research*, 95(D6), 7553. <https://doi.org/10.1029/JD095iD06p07553>

US Department of Commerce, N. E. S. R. L. C. S. D. (n.d.). FIREX Fire Lab 2016. Retrieved from <https://www.esrl.noaa.gov/csd/projects/firex/firelab/>

US EPA, O. (n.d.). NAAQS Table. Retrieved from <https://www.epa.gov/criteria-air-pollutants/naaqs-table>

Veres, P., Roberts, J. M., Burling, I. R., Warneke, C., de Gouw, J., & Yokelson, R. J. (2010). Measurements of gas-phase inorganic and organic acids from biomass fires by negative-ion proton-transfer chemical-ionization mass spectrometry. *Journal of Geophysical Research*, 115(D23), D23302. <https://doi.org/10.1029/2010JD014033>

Warneke, Carsten, Roberts, J. M., Schwarz, J. P., Yokelson, R. J., Pierce, B., De Gouw, J. A., ... Fahey, D. W. (2015). Fire Influence on Regional and Global Environments Experiment Fire Influence on Regional and Global Environments Experiment (FIREX) Motivation and Objectives. Retrieved from <https://www.esrl.noaa.gov/csd/projects/firex/whitepaper.pdf>

Warneke, Catsten, Ahomadov, R., & O'Neill, S. (n.d.). Session Proposal: Fire's Impact on Air Quality and Climate - Measurements and Predictions Across All Scales (2017 AGU Fall Meeting). Retrieved February 6, 2018, from <https://agu.confex.com/agu/fm17/preliminaryview.cgi/Session29194>

## Appendix A

### A.1 Detailed Examination of 10 through 16 August

#### A.1.1 10 – 11 August (Figure 9)

Stationary sampling took place at Wagon Hammer RV Park in North Fork ID from 10–12 August, 70 km North of the RFF. During this time interval the prevailing winds blew from the NE and we sampled a relatively old air mass (calculated using the methods in §2.4 as 30-60 hours).

The HONO concentrations from 12:27-16:01 (Figure 10; blue) remained relatively constant, between 50 and 100 pptv. HNO<sub>3</sub> levels were more erratic during this time interval, ranging between 50 and 175 pptv (Figure 10; red). The ratio of HONO/HNO<sub>3</sub> averaged around 0.6 (Figure 10A). At 16:14 HONO increased to 145 pptv, and HNO<sub>3</sub> began a slow decline from 231 pptv to 10 pptv the next morning ~04:00. After the initial jump in concentration from 145 pptv, HONO levels were highly variable and the ratio of HONO/HNO<sub>3</sub> climbed from ~0.6 to 13, following an erratic behavior like the HONO concentrations.

#### A.1.2 12 – 13 August (Figure 10)

On the drive from North Fork to Royal Gorge, the van passed through a visible smoke plume from the RFF between 10:40 and 12:35 (Fig 11). The wind was blowing from the South towards the van at this time, and plume age was estimated at approximately 1-2 hours. HONO concentrations increased from 50 pptv to ~600 pptv in the first visibly thicker parcel of smoke impacted air (10:40-11:40). The HONO/HNO<sub>3</sub> ratio averaged 4.2 during this interval. From 12:00-12:35 HONO concentrations were maintained near 150 pptv, and the HONO/HNO<sub>3</sub> ratio averaged 1.5 reflecting both the smaller HONO enhancement and a steady increase of HNO<sub>3</sub> concentrations. After passing into visibly clearer air the HNO<sub>3</sub> and HONO levels remained roughly constant until ~20:00, and the HONO/HNO<sub>3</sub> ratio averaged 0.42. These relatively consistent concentrations, with a few visible spikes and dips, occurred over several periods of stationary and mobile measurements. At 20:00 HNO<sub>3</sub> steadily decreased to 20 pptv before increasing again to 35 ppt between 0:00-4:00, while HONO remained near 50 pptv.

At 04:00 on 13 August mobile measurements began on highway 93 between Ellis and Challis. We encountered thick smoke at 04:47 - 05:00 near the intersection with MCR, marked by a HONO spike reaching 235 ppt and an average HONO/HNO<sub>3</sub> ratio of 18.0, in contrast to values of 4-6 before and after we intercepted the plume. At 05:54 the van turned up MCR, encountering a larger HONO enhancement of 368 pptv, and average ratio of 56.2, in a pulse of smoke which lasted until 06:15. From 06:28 until 07:17 the van climbed MCR and drove closer the RFF. While the van never reached the barricade marking the area closed by the Forest Service, our team collected two samples estimated to be 7-10 km from the flame front of the RFF. As noted in the fire history, the fire actively grew toward MCR throughout 13 August, consuming upwards of 8,000 acres of land. (Figure 4). The concentration of HONO was > 600 pptv from 06:35 – 07:50 and peaked at 1100 pptv. The HONO/HNO<sub>3</sub> ratio averaged 64.4

during the prior defined time interval. In the two samples collected when the van stopped at closest point to the RFF on this mobile run, the ratios were 165 and 145, with HONO concentrations at 893 and 870 pptv respectively. The ratios in these two samples are the largest in the campaign, driven mainly by the low concentrations of HNO<sub>3</sub> (on the order of 50 pptv) rather than extreme levels of HONO. The high average value of the ratio also reflects the relatively small (~50pptv) enhancements in HNO<sub>3</sub> during the ascent and descent of MCR. The age of smoke at closest approach was estimated to be 3.5 hours, with a range of smoke ages from 2 to 6 hours throughout the time spent on MCR during the early morning 13 August. The nocturnal inversion lifted during this time, resulting in clearer air and more distinct and defined plume edges, as noted by the Forest Service in their twice daily updates. The mobile laboratory returned to Royal Gorge at 09:00 and the MC/IC was shut down for recalibration.

#### A.1.3 13 – 14 August (Figure 11)

After recalibration, the MC/IC conducted stationary sampling at Royal Gorge from 11:40 – 22:20. The wind came primarily from the East, bringing well-aged air masses likely impacted by the Goldstone Fire, ~ 40 km NE of Royal Gorge. HONO concentrations were slightly enhanced, staying below 100 pptv except for 4 small spikes less than 150 pptv. HNO<sub>3</sub> levels increased from ~75 pptv to ~150 pptv. During this period of increasing HNO<sub>3</sub> concentrations, the ratio of HONO/HNO<sub>3</sub> remained low, with an average of 0.46. At 18:46 HNO<sub>3</sub> levels began to steadily decrease to 50 pptv by 22:00, and HONO decreased from 50 to 20 pptv.

Mobile measurements began at 22:20, and upon pulling out of the shallow Royal Gorge valley, we were inundated with smoke, easily detectable by smell and visual haze, helping to guide our movements. If we stopped smelling smoke or seeing haze, we turned around, and retraced our previous movements until we smelled, and saw smoke again. Within forty minutes of leaving Royal Gorge, HONO concentrations rose to over 600 pptv, while HNO<sub>3</sub> concentrations remained under 100 pptv, and the HONO/HNO<sub>3</sub> ratio grew from 0.4 to 8. We drove up MCR and reached the forest service barricade at 23:26 and sampled for ~7 minutes. It is important to note that the Forest Service expanded the closure area around RFF during 13 August, moving the barricade 4 km further down the road than where the van had turned around early that morning. After the sample collection, we drove back to ID-93. While on MCR HONO levels rose to a max value of 751 pptv, and HNO<sub>3</sub> concentrations varied, with a maximum of 93 pptv and minimum of 26 pptv. The HONO/HNO<sub>3</sub> ratio fluctuated between 6 and 8, with two major jumps to 17 and 24. After returning to ID-93 we turned south and drove towards Challis and onto Challis Creek road around 00:20 where HONO levels stayed elevated between 300 and 450 pptv, and HNO<sub>3</sub> levels ranged between 60 and 95 pptv.

Upon turning onto Challis Creek Road, we saw a small dip in HONO levels, down to 300 from ~450 pptv, punctuated by a sharp decrease over two samples to 63 and 80 pptv respectively. HNO<sub>3</sub> levels rose slightly while up Challis Creek Road, from 56 pptv to 95 pptv, with the HONO/HNO<sub>3</sub> ratio trending downward from 10 to 1 at the furthest point up Challis Creek road. After we turned around and drove back towards ID-93, the ratio increased to 4-7. We returned to MCR at 01:50 and saw an increase in HONO levels to ~450 pptv, with two spikes at 573 and 517 pptv. HNO<sub>3</sub> was between 60 and 80 pptv, lower than the previous MCR

runs, resulting in HONO/HNO<sub>3</sub> ratios of 4-6. At 02:50 we descended MCR again and headed back towards Royal Gorge for a driver change.

Trends of the two species while on ID-93 this second time mirrored those seen on ID-93 driving between MCR and Challis Creek Road. At Royal Gorge at 03:17, HONO levels went down dramatically, to 65 pptv, and HNO<sub>3</sub> levels rose to 77 pptv, driving down the ratio to 0.8. The van remained stationary at Royal Gorge until 03:40, when the second team made measurements between Royal Gorge and Challis for two hours. HONO and HNO<sub>3</sub> levels stayed relatively low for this portion of mobile measurements, with one major HONO spike at 05:34. HONO levels stayed between 150 and 230 pptv, HNO<sub>3</sub> between 25 and 30 pptv, and HONO/HNO<sub>3</sub> ratios between 6 and 10. During the HONO spike the van was driving North towards Royal Gorge from Challis and intercepted an air parcel of fresh smoke, ~3 hours old, being blown SW from the RFF. It is important to note the high variability in the HONO and HNO<sub>3</sub> concentrations during this period of sampling. Increases and decreases in the two species are sometimes in phase, and sometimes out of phase with one another. Based on Forest Service reports there was strong inversion layer present this night that trapped the smoke in the valley, blurring the edges of individual plumes and increasing the variability of the concentrations of the two species.

Upon returning to Royal Gorge at 06:00, we made stationary measurements for the remainder of the morning, until 11:52. HONO levels during this interval stayed between 150 – 200 pptv and HNO<sub>3</sub> stayed below 50 pptv until 09:30, when HONO dropped below 100 pptv and HNO<sub>3</sub> began a steady rise to 140 pptv. During this stationary interval, the HONO/HNO<sub>3</sub> ratio steadily dropped from 7.5 to 0.45.

#### A.1.4 14 -15 August (Figure 12)

On August 14<sup>th</sup> the RFF grew 7,000 acres, from 16,000 acres to 23,000 acres; reported as one of the largest days of growth for the fire, as seen in Figure 4, and Figure 7, in the transition from yellow to orange area, delineated by the black and blue lines. Most of the growth of the RFF occurred on the upper NE side of the fire, with smaller growth happening on the southern end, close to the Spike Camp.

A smoke impacted air mass was intercepted on the afternoon 14 August while the van was stationary at Royal Gorge, with one small excursion north to attempt to find more dense smoke. This air mass blew from the NE and was roughly 3-5 hours old. While stationary at Royal Gorge (16:43 – 17:30), HONO concentrations increased from 50 pptv to 230 pptv, HNO<sub>3</sub> increased from a background level around 190 pptv to 488 pptv, and the HONO/HNO<sub>3</sub> ratio stayed relatively constant between 0.32-0.46. The brief stint of mobile measurements from 17:37 – 17:50 corresponds to a dip in HONO and HNO<sub>3</sub> concentrations, showing that our attempts to infiltrate thicker smoke were unsuccessful. In the second parcel of more strongly impacted air observed while stationary back at Royal Gorge (17:50 – 18:38) HONO concentrations increased from 75 pptv to 323 pptv and HNO<sub>3</sub> increased slightly from 270 pptv to 338 pptv. The HONO/HNO<sub>3</sub> ratio from 0.27 to 1, driven upwards by the proportionally larger increase in HONO. Once the impacted air mass passed over Royal Gorge, HONO levels stabilized between

20 and 40 pptv, HNO<sub>3</sub> levels slowly decreased from 338 to 50 pptv over the course of several hours (18:17 – 22:34). The HONO/HNO<sub>3</sub> ratio increased as HNO<sub>3</sub> decreased, from 0.18 to ~0.8.

Mobile measurements began at 23:22, encountering smoke as the van passed the junction of MCR and ID-93. Five passes were made across the MCR/93 junction from the start of mobile measurements until 02:22 on 15 August. These passes are marked by HONO enhancements up to 693, 613, 562, and 392 pptv, respectively, from a baseline near 35 pptv. HNO<sub>3</sub> levels showed the same trend, spiking in phase with the HONO spikes, 30-50 pptv on top of a 30 pptv baseline. The HONO/ HNO<sub>3</sub> ratio in the MC drainage increased to 7.9, 7.4, 7.2, 5.9, 5.4, and 7.5 in the successive crossings, above a baseline averaging 4.7. After making the passes by the mouth of MCR, we turned up the road and drove to the barricade (02:20- 03:30) and made stationary measurements until 04:10, before returning to Royal Gorge for a driver exchange. During the drive up MCR, HONO generally increased, peaking at 1650 ppt, but oscillated between samples by several hundred pptv. Nitric acid covaried with HONO, peaking at 132 pptv with proportionately smaller variations between samples. At the barricade HONO ranged 1547 – 1873 pptv and HNO<sub>3</sub> ranged 129 – 204 ppt. On the drive back down to 93 variations in both acids basically mirrored the pattern seen on the ascent. During the entire period the van was on MCR the HONO/HNO<sub>3</sub> ratio ranged 8.2 – 12.5 (average 11.5), with no obvious enhancement during the stationary sampling at the barricade. The smoke was tentatively estimated at 6-11 hours old, but winds were gusty and variable, making these estimates uncertain. Back on the highway heading to Royal Gorge HONO and HNO<sub>3</sub> concentrations returned to background levels around 120 pptv and 30 pptv respectively.

After we exchanged drivers, the new crew returned to the barricade up MCR from 05:46 to 07:34. During this time we saw similar enhancements in HONO (2052 pptv) and HNO<sub>3</sub> (177 pptv). However, these enhancements occurred out of phase, with HNO<sub>3</sub> peaking twenty minutes after HONO. The HONO/HNO<sub>3</sub> ratio varied between 6 and 14. The air sampled here was slightly younger, ~5-6 hours old, and wind was blowing more consistently from the SW, towards our location. At 07:01 the van began to drive back down towards 93, arrived in Challis at 07:35, and remained there until 09:00, at which point the MC/IC had to be shut down due to low eluent levels and the van returned to Royal Gorge for recalibration.

#### A.1.5 15 – 16 August (Figure 13)

After recalibration, mobile measurements were made between Salmon and Royal Gorge during the afternoon (12:07 - 15:57). We targeted sampling along this stretch of ID-93 because the WE-CAN C-130 was scheduled to fly over Salmon and we wanted to intercept it. The drive from Royal Gorge to Salmon was characterized by fluctuating HONO levels between 60 – 160 pptv (12:07-13:00), and equally variable changes in HNO<sub>3</sub> concentrations, between 128-286 pptv. The spikes in concentration for the two species were out of phase and the HONO/HNO<sub>3</sub> ratio varied between 1.5 and 5. The wind was sweeping the smoke directly across ID-93, blowing from the SW, from the RFF, with age of emissions estimated to be ~5-10 hours. Once in Salmon the van remained stationary (13:06 to 13:42), marked by equally variable concentrations in both HONO and HNO<sub>3</sub>. At 13:50 the van began the drive to Challis. The wind continued to blow from the SW, with S/SE gusts, shifting at 15:49 to winds from the W/NW. Large HONO

enhancements peaking at 458 pptv were seen during this southward drive, where plumes averaged 1-3 hours old, with intermittent parcels of more aged air, 4-7 hours old. During this southward drive to Challis HNO<sub>3</sub> peaked at 250 pptv, seven minutes before the HONO spike. The highest ratio of the two species seen in this interval was 2, and it averaged around 1. The van reached Challis at 15:32 and immediately started the return trip to Royal Gorge. On this leg of the trip the MC/IC suffered a burst eluent line and was taken offline for repairs between the hours of 16:00 and 19:00 and the van returned to Royal Gorge

After repairs the MC/IC resumed measuring at 19:36, stationary at Royal Gorge for the remainder of 15 August and into the morning of 16 August. HONO levels remained constant and low between 16 pptv and 26 pptv while HNO<sub>3</sub> concentrations slowly declined from 116 pptv to 42 pptv. The ratio of the two species slowly increased from 0.1 to 0.9. Around midnight, HONO levels suddenly increase from 26 pptv to 130 pptv over a 2-hour period, remaining close to 130 pptv until 08:05. HNO<sub>3</sub> continued its slow decrease to a low of 17 pptv, and the HONO/HNO<sub>3</sub> ratio increased from 0.9 to 6. At 08:00 HONO levels begin to fall, and HNO<sub>3</sub> levels start to increase. The ratio of the two species fell from 6 to 2.

#### A.1.6 Daytime Spike Camp Measurements on 16 August (Figure 14)

On 16 August, daytime measurements were made in fresh smoke at Spike Camp, past the barricade on MCR where we had previously been sampling. This was the closest approach to the RFF we were able to achieve, at 10.7 km from the fire start and 2 km from the fire line. At 14:56 we left Royal Gorge and drove to MCR arriving at Spike Camp at 16:02. During the drive to Spike Camp the air we were sampling decreased drastically in age, from 15 hours to under 1 hour old. This shift occurred as we drove up MCR into fresher air parcels as we gained in elevation. The prevailing winds blew from the N/NE, from the RFF directly towards Spike Camp. As we approached Spike Camp HONO concentrations became more variable, fluctuating between 60 and 180 pptv and HNO<sub>3</sub> concentrations decreased from 150 pptv to 60 pptv. The ratio of HONO/HNO<sub>3</sub> stayed between 0.5-1 for the duration of the climb, varying with the spikes and dips in HONO concentration.

While we were stationary at Spike Camp, from 15:57 pm – 18:00 pm, 3 different puffs of smoke mixed down to the van, visualized by the spikes in HONO concentrations. These spikes reached 400, 519, and 725 pptv of HONO. Corresponding HNO<sub>3</sub> concentrations were 91, 76, and 57 pptv, and generally represented decreases in the HNO<sub>3</sub> concentration. The HONO/HNO<sub>3</sub> ratio in the successive puffs of thick smoke were 4, 6.8, and 13, compared to 1.5 during the rest of stationary sampling at Spike Camp. As we began our descent down MCR and back into more aged smoke, the HNO<sub>3</sub> concentrations rose back to daytime levels between 120 and 180 pptv, and HONO decreased to below 100 pptv, and even below 50 pptv for several consecutive samples. The HONO/HNO<sub>3</sub> ratio decreased to 0.2-0.4. At 19:08 we encountered a BB impacted air mass on ID-93 as we drove towards Royal Gorge. HONO spiked to 332 pptv for one sample, while HNO<sub>3</sub> dropped from 170 pptv to 118 pptv. We returned to Royal Gorge at 19:39 and measured a smaller HONO spike of 264 pptv and corresponding drop in HNO<sub>3</sub> levels from 120 pptv to 80 pptv. Both small HONO spikes occur in air masses ~2 hours old, separated by air that

is closer to 14 hours old. Between 20:00 and 22:00 hours,  $\text{HNO}_3$  decreased to night levels around 50 pptv while HONO levels began to slowly build.